RESPONSE TO ANONYMOUS REFEREE #1

Referee: At first I want to apologize for the delay of my review. The paper by Pietrodangelo et al. analyses the composition, size distribution, optical properties and radiative effects of local resuspended dust particles in the area of Rome. The paper is well written and all the laboratory analyses are performed with following a rigorous approach. The results indicate several differences in the chemical composition/size distribution of the resuspended dust which is discussed to play a role in modulating the particle optical properties and radiative effects in the area of Rome.

Authors: The authors are grateful to the Anonymous referee #1 for helpful suggestions and remarks concerning the Manuscript acp-2015-259, which allowed to improve consistently the scientific quality of this study. All suggestions from the Referee have been followed, and remarks have been discussed extensively, as follows.

R: The paper has potentially the interest for publication on ACP, however I have several major concerns, which are listed below:

1. Concerning the introduction/context: I have some problems in identifying the importance of the study in link to the mean aerosol composition/optical depth in the area of Rome. Which is the fraction of PM10 that can be associated to resuspended dust in the area of Rome? Which is the frequence of occurrence of these episodes and their impact on the visible optical depth?

A: The *reviewer* addresses an *interesting question about the role of local mineral dust of Rome area on the PM_{10} and on the impact of this contribution on the visible optical depth*. On the basis of this query, the following considerations can be made.

1. Some comments, on the frequency and the influence on the mass concentration, of local crustal dust resuspension to the ambient PM_{10} in the Rome area have now been added in the Introduction, and two figures (Figures 2S and 3S) have been added to the Supplementary materials (Supplementary materials_revised), to support the discussion on this item. To summarize briefly, a long period has been analysed (2005 ï 2011 and 2005 ï 2015, depending on the site), for which data are available at two different background sites in Rome area (as showed in Figures 2S and 3S). The goal was to evaluate the number of days and the entity of the crustal contribution, on days of desert dust intrusion at-ground (DD-days) and on days showing a large crustal contribution (above 50% of total PM_{10} mass) without occurrence of desert dust at-ground, indicating a crustal contribution from local sources (LD-days). Interestingly, among the above described days, the mass concentration of the crustal matter on LD-days is in many cases comparable with that observed on DD-days.

2. The local mineral dust samples of this study have to be considered as emitted at source, as discussed in the following points. The visible optical depth due to these samples is thus negligible with respect to the columnar AOD.

In fact, the AOD of these components is not directly comparable to the c*olumn* integrated AOD measured during the local dust events, the reason of which is discussed in the reply to question #2. To this aim, the authors have been analysed the AOD downloaded from the Rome Tor Vergata AERONET station nearest to the recognized sources. The AOD@532nm is generally between 0.2-0.3 with Angstrom coefficient larger than *one*, *fine* mode aerosols *dominate* the atmospheric column. As example, the Figure shows the AOD@532nm and the Angstrom coefficient for two events of local and Saharan dust, respectively.

Local Dust	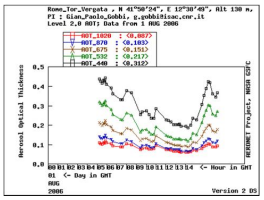	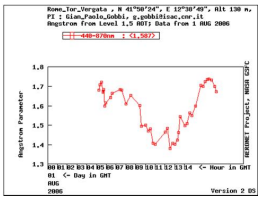
Saharan Dust	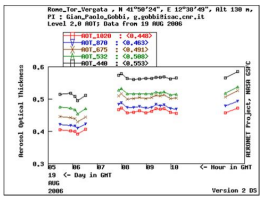	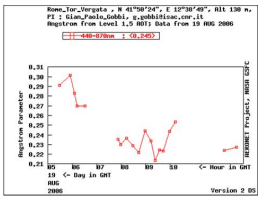

Therefore, following the reviewerôs suggestions, *to evaluate the radiative efficiency of the local dust*, the radiative impact of the principal components of the chemical mixture, travertine and volcanic, independently from their loading has been evaluated introducing the efficiency radiative forcing. This allows us to achieve manuscript *purposes* with results not related to the influence of these components to the total visible optical depth. Furthermore, the PM_{10} samples of this work are obtained from topsoil/outcropped rocks materials collected at the source, while the available radiative measurements are not close to these sites. Under this aspect, the AERONET data cannot be considered as representative of the local dust spread on the Rome area and, therefore, cannot be compared with the dust samples of this work.

R: 2. Concerning the representativeness of the considered samples: how the size distribution of the analysed samples is representative of airborne particles? And for the mineralogy?

A: The approach of laboratory resuspension of dust by mechanical ventilation along an adequate time and by simultaneous sampling in the controlled environment of the chamber, is widely employed in the research field of the mineralogical and microphysical characterization of airborne crustal dust (e.g. Gill et al., 2006 and references therein; Feng et al., 2011; Aimar et al., 2012; Dobrzhinsky et al, 2012). By this approach, indeed, it is possible to reproduce with good approximation the conditions of the field sampling at a dust source, and the size distribution of the resuspended particles is negligibly affected, with respect to the original distribution in the source material. This is extensively treated by Gill et al. (2006). Moreover, it should be taken into account that the PM10 samples of this work are obtained by a PM10 sampling head compliant with EN12341 standard (as reported in the paper by Pietrodangelo et al., 2013, cited in Section 2.1 of the Manuscript). Therefore particles in the samples of this work have aerodynamic diameter below 10µm and can be considered, with sufficient approximation, as if they were collected at the dust source. To better clarify this point, some comments have been added in Section 2.1 of the revised Manuscript (p.5, lines 23 ï 31).
Under the above arguments, the mineralogy of the PM10 particles collected by chamber resuspension in this study can be considered representative of the mineralogy of the same particles in the geological source materials. The approximation by which this assumption is made depends strictly on the confidence on the ability of this approach in reproducing the conditions of field sampling at a dust source, as above discussed, at least with respect to the interference of the PM10 sampler on the dust source itself. Considering that about 95% of mineral particle included in this study show physical size below, or equal to, 5 µm, our results

are also in line with arguments reported by Mahowald et al. (2014): *ñAccurate representation of the dust particle size distribution (PSD) in the atmosphere begins with a parameterization of the dust PSD at emission. Note that the different measurements of the size distributions at emission are all in rough agreement for dust aerosols smaller than 5 µm in diameter é . This is quite remarkable, considering that these measurements were taken over different soils, in different source regions, and using different techniques. For larger particles (> 5 µm), the size distributions do differ substantially, a possible cause of which is discussed in the next section. In order to parameterize the dust PSD at emission in models, the dependence on wind speed and soil properties, such as soil PSD, needs to be understood. A number of studies have reported measurements of the dust PSD at different values of the wind friction speedé . Most of these measurements show no dependence of the dust PSD on the wind speed at emission éé .*
On balance, the measurements indicate that the dust PSD is independent of the wind speed at emission. This conclusion is supported by the observation of Reid et al. (2008) that the PSD of dust advected from individual source regions appeared invariant to the wind speed at emission.ò

R: 3. What about the obtained mineralogical composition in comparison with that of similar sources? It is possible to have a comparison with other studies?

A: The availability in literature of dust sources similar to those investigated in this study is small, due to the peculiar geological setting of the Latium region, and in particular of Rome area, as widely discussed in the paper by Pietrodangelo et al. (2013), which is cited in Section 2.1 (p.6, line 2 of the revised Manuscript) concerning this point. Moreover, given the great effort of experimental work required to determine quantitatively the mineralogical composition of the airborne PM, few studies concern this aspect (as reported at p.4, lines 3-7, of the revised Manuscript). Nevertheless, we can add to the already cited references the mineralogical profiles of PM10 from mineral dust sources located in North Africa and Saudi Arabia (Ganor et al., 2009). We discussed this reference adding some text in Section 3.4.1.

R: 4. Concerning the calculation of the optical properties, I do not agree with the fact that calcite is not absorbing; conversely, in the shortwave, calcite is one of the most absorbing minerals. I think you have to reconsider the choices of the refractive indices for your minerals/samples. Moreover, considering that you have measured the mineralogy, why not calculating the complex refractive index based on the mineralogical composition using either and internal mixing or external mixing rule?

A: Calcite is absorbing significantly above 5000 nm. The imaginary part of the refractive index (r.i.) is, in the wavelength range considered by our study, below 0.01 (Sokolik & Toon 1999, Di Biagio et al. 2014). Moreover, the calculation of the complex r.i. (e.g., as performed by Kandler et al., (2007) at 550 nm only) is out of the aims of our study, since the radiative transfer code 6SV requires, among other inputs, the spectral trend of the real and of the imaginary parts of the r.i. in the range 350 ï 3750 nm. Concerning the volcanics sample, it was not possible to build the real and imaginary parts of r.i. on the basis of the mineralogical composition determined, e.g. introducing a complex mixing model, due to the lack of numerical data, in literature, in the wavelength range required for simulations by the 6SV code. Indeed, the availability of the spectral trend of the imaginary part of r.i. is limited to 2500 nm for most minerals. Moreover, available spectral data of the r.i. account only for ab.

70% of the mineralogical composition of the volcanic sample; the uncertainty which would be introduced by not considering mineral phases, such as plagioclase and pyroxene, for which appropriate data are not available in literature, would be thus too large to apply a complex mixing modelling to estimate the r.i.. Therefore, the choice of assuming the r.i. spectral trend of the ñwater-insolubleò aerosol component provided by the 6S radiative model, which is rich in silicate minerals similarly to the volcanics dust of this study, was considered more suitable. The authors are anyway grateful to the Reviewer for the suggestion of introducing a complex mixing model, and aim at developing this issue in future studies.

R: 5. Concerning the presentation of the study, I find that the text is too long and that there are too many experimental details both in the measurements section and in the results section. I would suggest to reorganize the paper considering moving some technical parts to Appendix.

A: Following the Reviewerôs suggestion, the detailed description of the internal standard approach used in this work to quantify particle elemental composition from SEM XEDS microanalysis has been removed from the Manuscript and added to the Supplementary materials, as Appendix I.

Specific comments

R: Abstract: define **BOA** here. Add also some **ñ**numbers**ò** in the Abstract, i.e. concerning the radiative effect or the optical properties.

A: The BOA has been explained in the text. The values of the radiative forcing efficiency have been added in the manuscript, -292.9 +/- 17.8 W/m2 for volcanics and -139.0 +/- 6.8 W/m2 for travertine.

R: Page 13349, lines 25-26: the indirect effect is not linked to the ñwarming or cooling of the atmosphereò, please correct.

A: The sentence on indirect effects has been corrected from ***ñ****warming or cooling of the atmosphere****ò*** to ***ñ****cloud-aerosol interactions****ò***.

R: You missed the reference by Rodriguez et al. (2012) in the reference list.

A: It was an error to keep this reference in the original Manuscript, maybe deriving from a sentence which has been deleted in the final version. The above reference is not present in the revised Manuscript.

RESPONSE TO ANONYMOUS REFEREE #2

Referee: The manuscript shows interesting results of measurements in an area little explored. Composition analysis was well done, combining different complementary methodologies. However, the authors made strong hypothesis without enough justification and thus the main conclusions are not as strong. Beside, manuscript english writing needs improving in some points.
Although the paper has potential interest for the ACP audience, I find it in need of major changes.

Authors: The authors would like to thank the Anonymous Referee #2 for helpful suggestions and remarks, which have been followed in most cases, in the revised Manuscript.

R: My concerns are:

1) R: Calibration of SEM XEDS are not shown nor referenced from another paper. Reliability is only accessed by comparison with EDXRF, for which the calibration was not shown/discussed as well. If they used NIST standard for calibration, or a different one, should be clarified.

A: Scanning Electron Microscopy combined with X-ray energy dispersive (XEDS) microanalysis requires calibration of the electron column, for morphological measurements, and of the energy dispersive spectrometer, for XEDS microanalysis. Differently from other analytical instruments, like EDXRF, both procedures are not performed on daily, or anyway frequent, basis, since a periodical (about every 3 ï 6 months) recalibration is sufficient to maintain the reproducibility of signals (mainly: secondary electrons, backscattered electrons and X rays emitted from sample), especially if samples from the same type of matrix are analysed, on routine. This is also the case of the Philips XL30 ESEM employed in this study, as by this instrument particulate matter samples collected on filter membranes are almost exclusively analysed, on laboratory routine. This is also the reason why neither calibration details are generally reported in the scientific literature on SEM XEDS microanalysis of environmental particulate matter, nor calibration curves are reported as well. Nevertheless, a short sentence has been added in the text of revised Manuscript (Section 2.2) indicating that the calibration procedures are in line with the US EPA Guidelines (2002) on the application of SEM XEDS microanalysis to particulate matter samplers. Moreover, it should be considered that quantification methods properly targeted on the SEM XEDS microanalysis of individual particles from environmental matrices does not exist, as discussed in the Manuscript (Section 2.3), and standard materials of environmental particulate matter properly dedicated to the quantification of the elemental composition of individual particles (relating to individual particles from environmental matrices) are not available. For this reason, the authors applied an internal standard approach to achieve the goal of quantification of particle elemental composition, which is an unavoidable step in the analytical structure of this study, and assessed the reliability of this approach (and of the procedure of particle allocation to mineral classes) by comparison with the quantitative results of elemental composition obtained by EDXRF on the bulk PM10 dust samples. Finally, given the above considerations, the term ósemi-quantificationô(and related terms) is more appropriate than quantification, in the case of SEM XEDS individual particle microanalysis applied to environmental matrices.

2) R: PCA cannot be used for the proposed analysis because it allows negative mass/concentration. The reference method in case is PMF (positive matrix factorisation).

A: In this work the PCA is employed to discuss results of the elemental ratios obtained by SEM XEDS microanalysis of individual dust particles; no limitation exists, to the authorôs knowledge, in applying the PCA to this type of data. The term ópartitionmentô in this study was used to indicate the assignation of each dust particle to the proper mineral group, and not referring to the field of the source apportionment (where Chemical Mass Balance, Multilinear Engine, and Positive Matrix Factorization models, are reference methods). As a matter of fact, indeed, mass apportionment is neither presented nor discussed all over this work. Mass data have been treated by a mass closure approach in Section 3.3, on the results of the assignation procedure, to the goal of assessing the reliability of this procedure versus the quantitative determination of the mineralogical composition by XRD. For sake of clarity, the term ópartitionmentô has been replaced by the term óassignationô (and related verb) in the revised Manuscript.

3) R: Discussion on size distribution is problematic because samples were produced in the lab. Authors did not mention, nor discussed if their method of resuspensions actually reproduce the same size distribution as would be measured in the atmosphere.

A: The focus of this study is the characterization of PM10 mineral dust at the dust source, and not in the atmosphere. This has been better clarified in the revised Manuscript. The approach of laboratory resuspension of dust by mechanical ventilation along an adequate time and by simultaneous sampling in the controlled environment of the chamber, is widely employed in the research field of the mineralogical and microphysical characterization of airborne crustal dust (e.g. Gill et al., 2006 and references therein; Feng et al., 2011; Aimar et al., 2012; Dobrzhinsky et al, 2012). By this approach, indeed, it is possible to reproduce with good approximation the conditions of the field sampling at a dust source, and the size distribution of the resuspended particles is negligibly affected by the laboratory procedure, with respect to the original distribution in the source material. This is extensively treated by Gill et al. (2006). Moreover, it should be taken into account that the PM10 samples of this work are obtained by a PM10 sampling head compliant with EN12341 standard (as reported in the paper by Pietrodangelo et al., 2013, cited in Section 2.1 of the Manuscript). Therefore particles in the samples of this work have aerodynamic diameter below 10µm and can be considered, with sufficient approximation, as if they were collected at the dust source. To better clarify this point, some comments have been added in Section 2.1 of the revised Manuscript. Under the above arguments, the mineralogy of the PM10 particles collected by chamber resuspension in this study can be considered representative of the mineralogy of the same particles in the geological source materials. The approximation by which this assumption is made depends strictly on the confidence on the ability of this approach, as reported in literature, of reproducing the conditions of field sampling at a dust source, as above discussed, at least with respect to the interference of the PM10 sampler on the dust source itself.
Considering that about 95% of mineral particle included in this study show physical size below, or equal to, 5 µm, our results are also in line with arguments reported by Mahowald et al. (2014): ***ñ****Accurate representation of the dust particle size distribution (PSD) in the atmosphere begins with a parameterization of the dust PSD at emission. Note that the different measurements of the size distributions at emission are all in rough agreement for dust aerosols smaller than 5 µm in diameter* ***é*** *. This is quite remarkable, considering that these measurements were taken over different soils, in different source regions, and using different techniques. For larger particles (> 5 µm), the size distributions do differ substantially, a possible cause of which is discussed in the next section. In order to*

parameterize the dust PSD at emission in models, the dependence on wind speed and soil properties, such as soil PSD, needs to be understood. A number of studies have reported measurements of the dust PSD at different values of the wind friction speedé . Most of these measurements show no dependence of the dust PSD on the wind speed at emission é é .
On balance, the measurements indicate that the dust PSD is independent of the wind speed at emission. This conclusion is supported by the observation of Reid et al. (2008) that the PSD of dust advected from individual source regions appeared invariant to the wind speed at emission.ò

4) R: All the discussion / conclusion on the RT calculations are simple direct implications of the ADHOC index of refractions chosen from the literature.

A: The choice of adopting refractive index (r.i.) data from literature was driven by the fact that the 6SV code requires as input the spectral trend of the real and imaginary parts of r.i., and these measurements were not available from our laboratory. Concerning the volcanics sample, it was not possible to build the real and imaginary parts of r.i. on the basis of the mineralogical composition determined, e.g. introducing a complex mixing model, due to the lack of numerical data, in literature, in the wavelength range required for simulations by the 6SV code. Indeed, the availability of the spectral trend of the imaginary part of r.i. is limited to 2500 nm for most minerals. Moreover, available spectral data of the r.i. account only for ab. 70% of the mineralogical composition of the volcanic sample; the uncertainty which would be introduced by not considering mineral phases, such as plagioclase and pyroxene, for which appropriate data are not available in literature, would be thus large. Therefore, the choice of assuming the r.i. spectral trend of the ñwater-insolubleò aerosol component reported in Kokhanovsky (2008), which is rich in silicate minerals similarly to the volcanics dust of this study, was considered more suitable. Concerning travertine, finally, the assumption of r.i. of calcite from literature is explicable on the basis of the travertine mineral composition (at least 95% calcite), as discussed in the Manuscript.

The authors have added results about radiative effect by introducing the radiative forcing efficiency (RFE) for the travertine and volcanic to define better the role of the radiative transfer calculation in this work. In fact, the retrieval of RFE requires models for aerosol-free fluxes calculated *in situ* only from RT runs. Furthermore, the fluxes simulations are normalized to the aerosol optical thickness (RFE) to evaluate the radiative forcing of the two components of local dust independently from the aerosol loading.

R: Some specific suggestion to the authors follows bellow.
R: a) Modify the abstract and introduction to better state what your work is about and why it is important.

A: The abstract and the introduction have been revised following the Reviewerôs suggestion.

R: b) Use Aeronet data for comparision. There are many years of data from Rome and from L'Aquila and you could select periods when dust concentration was expected to be high. From the inversion you will have not only the size distribution, but also the asymmetry parameter and single scattering albedo... and even the real and imaginary parts of the refractive index!

A: Considering the goals of this work, declared by the authors, the AERONET data are not useful for any comparison. The AERONET data (size distribution, refractive index, asymmetry parameter, single scattering albedo..) are referred to the mixed aerosol in the atmospheric column. This basic characteristic of the measurements returns *column-integrated* products not comparable with the results of this work where the simulation has been performed under conditions related to an atmosphere where the only aerosol component is the PM_{10} mineral dust (volcanics or travertine, alternatively), at dust source. Furthermore, Rome Tor Vergata AERONET station is not close enough to the identified dust source, for considering AERONET products representative of microphysical and optical properties of the local dust. L'Aquila station is farer than the Rome station, increasing the distance and discarding the chance to consider the samples of the presented work as the coarse component of the products obtained from AERONET radiative measurements.

R: c) Use transmission or reflectance methods in the lab to measure the resuspended material deposited on the filters. That will give you scattering and absorption directly.

A: The reviewer suggests methods for radiative measurements which could be applied if appropriate equipment were available in laboratory; this is not the case of this work. For these reasons, the authors have applied an approach which allows to meet data and tools actually available and which is suitable for the aerosol optical properties and radiative effects evaluation, as declared in the goals of this work.

RESPONSE TO ANONYMOUS REFEREE #2 ï SUPPLEMENT

R: In the attached manuscript I tried to identify all the typos and points were attention is needed.

p. 13348 L. 1. R: As the first sentence of the abstract, this is a bit confusing.

A: The first sentence has been rephrased in: óIn this work, new information has been gained on the laboratory resuspended PM_{10} fraction from geological topsoil and outcropped rocks representative of Rome area, Latium. Mineral composition, size distribution, optical properties and the radiative efficiency of dust types representing the compositional end-members of this geological area have been addressedô.

p. 13348 L. 5. R: It is also unclear which techniques you applied to which type of aerosols.

A: ñA multi-disciplinary approach was used, based on individual-particle scanning electron microscopy with X-ray energy-dispersive microanalysis (SEM XEDS), X-ray diffraction (XRD) analysis of dust, size distribution of mineral particles, and radiative transfer modelling (RTM).The mineral composition of Rome lithogenic PM 10 varies between an end-member dominated by silicate minerals and one exclusively composed of calcite.ò
This sentence has been rephrased in:
ñA multi-disciplinary approach was used, based on chamber resuspension of raw materials and PM10 sampling, to simulate field sampling at dust source, scanning electron microscopy / X-ray energy-dispersive microanalysis (SEM XEDS) of individual mineral particles, X-ray diffraction (XRD) analysis of bulk dust samples, number and volume size distribution (SD) building from microanalysis data of mineral particles and fitting to Log-normal curve, and radiative transfer modelling (RTM) to retrieve optical properties and radiative effects.ò

p. 13348 L. 20. R: In the atmosphere? or did you resuspended in the lab some material collected in the field?

A: This point has been clarified in the revised Manuscript. Please refer also to reply to General concerns #3.

p. 13348 L. 25. R: please define the **acronym**.

A: ñBOAò has been defined ñBottom Of Atmosphereò.

p. 13348 L. 25. R: but have you actually measured particles with this composition in the atmosphere? how much in # and mass are their contribution?

A: ñThe downward component of the BOA solar irradiance simulated by RTM for a volcanics-rich or travertine-rich atmosphere shows that volcanics contribution to the solar irradiance differs significantly from that of travertine in the NIR region, while similar contributions are modelled in the VIS.ò The sentence has been re-written to better address that the simulation is performed assuming an atmosphere in which the only aerosol component is, alternatively, or volcanics PM10, or travertine PM10 dust. ñThe downward component of the BOA solar irradiance simulated by RTM for an atmosphere composed of pure volcanics and pure travertine shows that volcanics contribution to the solar irradiance differs significantly

from that of travertine in the NIR region, while similar contributions are modelled in the VIS.ò

Please refer also to reply to General concerns #3.

p. 13349 L. 1. R: not true in general. think for instance over the ocean, or over tropical forests. if this is true for continental europe or italy, please cite a reference.

A: ñAirborne geological dust from topsoil and surface rocks represents a critical contribution to the total mass, composition, microphysical and optical properties of the atmospheric aerosol.ò This sentence has been rephrased in: ñAirborne geological dust sourced from topsoil and surface rocks critically contribute to the total mass, composition, microphysical and optical properties of the atmospheric aerosol in continental regions, and largely impacts different Earthôs compartments by transport and deposition (Scheuvens and Kandler, 2014)ò.

p. 13349 L. 6. R: There are many other previous papers that showed complex organic molecules and mineral components in particulate matter. It is not a consequence of the occurrence of lithogenic dust.

A: This sentence has been deleted in the revised Manuscript.

p. 13349 L. 26. R: indirect effect refers to aerosol changes in the radiation balance through cloud-aerosol interactions.

A: ñAirborne lithogenic dust plays a role both in the direct mechanisms (light scattering and absorption) and in the indirect mechanisms (warming or cooling of the atmosphere) which tune the Earthôs radiative budget (Sokolik et al., 2001; Choobari et al., 2014).ò The sentence has been rewritten ñAirborne lithogenic dust plays a role both in the direct mechanisms (light scattering and absorption) and in the indirect mechanisms (cloud-aerosol interactions) which tune the Earthôs radiative budget (Sokolik et al., 2001; Choobari et al., 2014).ò

p. 13349 L. 28. R: If you are using "indirect effect" differently than current current scientific consensus (e.g. IPCC reports) then you should better properly define it.

A: Please refer to the reply to reply to previous comment.

p. 13350 L. 1. R: Cloud-Aerosol interaction can be affected IF heterogeneous chemistry happens on particle's surface, but it is not a necessary condition for it to happen.

A: ñWhile indirect effects depend on the heterogeneous chemistry occurring at particles surface (Levin et al., 1996; Buseck and Pósfai, 1999; Sokolik et al., 2001; Krueger at al., 2004; Kandler et al., 2007), the light scattering and absorption are mostly controlled by the mineralogical composition, shape features and microphysical properties of geological particles (DôAlmeida, 1987; Kalashnikova and Sokolik, 2002 and 2004; Kokhanovsky, 2008; Hansell et al., 2011).ò

The sentence has been re-written in: ñConsidering direct effects, airborne lithogenic dust plays a key role in the light scattering and absorption, which are mostly controlled by the mineralogical composition, shape features and microphysical properties of geological particles (DôAlmeida, 1987; Kalashnikova and Sokolik, 2002 and 2004; Kokhanovsky, 2008;

Hansell et al., 2011).ò

p. 13350 L. 22. R: please define or maybe rephrase (rain aggressiveness). please define (FFAO index).

A: ñLatium is also affected by high rain aggressiveness, within the scale of FFAO index, and is characterised by a large surface where poorly-developed soils and debris deposits are present, which are easily affected by massive erosionò.
This sentence has been deleted in the revised Manuscript.

p. 13350 L 25. R: you can expect, but if you do not measure in the atmosphere you will never know.

A: ñConsidering also the high anthropic impact on the Latium territory, it has to be expected that the re-suspension of mineral dust from local lithological domains is non- negligible in this region.ò

Following the Reviewerôs suggestion, this point has been further discussed in the revised Manuscript. Some comments, on the frequency and the influence on the mass concentration, of local crustal dust resuspension to the ambient PM_{10} in the Rome area have now been added in the Introduction, and two figures (Figures 2S and 3S) have been added to the Supplementary materials (Supplementary materials_revised), to support the discussion on this item. To summarize briefly, a long period has been analysed (2005 ï 2011 and 2005 ï 2015, depending on the site), for which data are available at two different background sites in Rome area (as showed in Figures 2S and 3S). The goal was to evaluate the number of days and the entity of the crustal contribution, on days of desert dust intrusion at-ground (DD-days) and on days showing a large crustal contribution (above 50% of total PM_{10} mass) without occurrence of desert dust at-ground, indicating a crustal contribution from local sources (LD-days). Interestingly, among the above described days, the mass concentration of the crustal matter on LD-days is in many cases comparable with that observed on DD-days.

p. 13351 L. 2. R: why not using **SFC (**surface**)** as it is more standard?

A: In literature, the radiative effects are referred as TOA for the Top Of Atmosphere and BOA for the Bottom Of Atmosphere, as reported in the NASA website for the AERONET inversion products:
http://aeronet.gsfc.nasa.gov/new_web/Documents/Inversion_products_V2.pdf

Codice campo modificato

p. 13351 L. 9. R: didn't you actually measured the size distribution of the particles in the atmosphere?

A: Size distributions have been obtained from the data set of SEM XEDS microanalysis of individual mineral particles of our samples, as discussed in the Manuscript. Please refer also to reply to General concerns #3. Furthermore, the sentence:
ñTo investigate relationships among these different aspects, a multi-faceted analysis was performed, on the basis of the following approaches: individual-particle scanning electron microscopy combined with X-ray energy-dispersive microanalysis (SEM XEDS), bulk mineralogical analysis by X-ray diffraction (XRD), parameterization of the size distribution to log-normal function, and radiative transfer modelling (RTM).ò has been rephrased in:

ñTo investigate relationships among these different aspects, a multi-faceted analysis was performed, on the basis of the following approaches: chamber resuspension of raw materials and PM10 sampling, to simulate field sampling at dust source, scanning electron microscopy / X-ray energy-dispersive microanalysis (SEM XEDS) of individual mineral particles, X-ray diffraction (XRD) analysis of bulk dust samples, number and volume size distribution (SD) building from microanalysis data of mineral particles and fitting to Log-normal curve, and radiative transfer modelling (RTM) to retrieve optical properties and radiative effects.

p. 13351 L. 17 R: This is not clear. Do you mean you collected 4km2 of samples? Or that all the sampling sites are located within 4km2? Or that each site is relatively uniform so that the sample is representative of at least 4km2 around the sampling position?

A: ñCollection areas of about 4 km were selected on the basis of criteria established after geological analysis of the Latium region, within main local geodynamics domains, namely: the volcanic complexes, the marine (limestones, marlstones and sandstones) deposits, the siliciclastic series (mainly flysch) and the quaternary deposits (mainly travertines).ò
This sentence has been rephrased in:
ñOn the basis of criteria established after geological analysis of the Latium region, the following geodynamics domains were considered: the volcanic complexes, the marine (limestones, marlstones and sandstones) deposits, the siliciclastic series (mainly flysch) and the quaternary deposits (mainly travertines).Sampling areas of about 4 km2 were selected within each local geodynamics domain; a number of dust collection points was identified, within each area, to obtain sub-samples of raw material, from which the final samples were obtained. The number of sampling areas varies within each domain, depending on the geographical extension and the geological complexity of the domainò.

p. 13351 L. 23. R: this should be clearly stated in the abstract and introduction.

A: ñPM_{10} dust was laboratory re-suspended from the bulk rocks samples, and from road dust, by a re-suspension chamber, and collected by low-volume sampling on polycarbonate membranes for SEM XEDS microanalysis.ò
This aspect has been clearly stated in the title, abstract and introduction.

p. 13353 L. 3. R: Launching?

A: ñlaunchò has been replaced with ñlaunchingò.

p. 13353 L. 8. R: Or?

A: ñandò has been replaced by the form ñboth onò, that is:

ñé .both on field areas and on individual particles, by using the EDAX control v. 3.3 package (EDAX Inc., 2000)ò.

p. 13354 L. 9. R: Secondary target?

A: The term ñtargetò has been added in this sentence:

óThe mineralogical characterization of dust samples has been carried out on the 50 µm sieved

dust fraction, by an automatic diffractometer Scintag X1, equipped with a Si(Li) detector using a Cu KŬtarget, é .ô

p. 13354 L. 28. R: At some point you should show the calibration curves for your instrument, or reference the paper where that was done.

A: This point has been extensively discussed in the reply to General concerns #1.

p. 13355 L. 20. R: This might not be clear enough for those who are not specialized on EDAX. We have an EDXRF in our lab., for instance, and it is not possible to get the matrix losses from the quantification routine itself.

A: The theory of microanalysis by SEM XEDS is widely treated in literature. The estimation of the Z (atomic number), A (absorption) and F (secondary fluorescence) factors to take into account the matrix effects is treated by the ZAF algorithm, which allows to improve quantification obtained by the application of the Castaingôs first approximation. The Z, A and F factors are commonly estimated in the sample matrix by the quantification routines included in the SEM XEDS software packages, based on the net intensities measurement of the X-rays spectrometer and on the specific instrumental parameters of each scanning electron microscope.

p. 13356 L. 6. R: Please clarifyé Do you mean total weight of the particle that could be identified < 50%?

A: The sentence related to this comment has been rephrased as:
òé .total percent weight (%wt) of the particle that could be identified below 50%....ò.

Please note that, following suggestions from the Anonymous Referee #1, the part of Section 2.3 concerning the internal standard approach to quantification of particle elemental composition, where the above sentence is placed, has been moved from the Manuscript to Appendix I (new) in the Supplementary materials.

p. 13357 L.3. R: But that is only representative of what you would observe in free atmosphere if your resuspension method precisely mimic nature. Do you have evidence that you method doesnôt prefer, for instance, to lift large particles in detriment of small particles?

A: We have experimental evidence that about 95% of particles included in this study have physical size below or equal to 5 µm; this is in line with literature on this issue (e.g. Gill et al., 2006 and references therein; Feng et al., 2011; Aimar et al., 2012; Dobrzhinsky et al, 2012), as extensively discussed in the reply to General concerns #3.

p. 13357, Log normal curve function. R: Why fitting the data instead of showing the measured sized distribution? Besides, why fig. 4 doesnôt look like a fitted size distribution?

A: The 6SV code requires, among other inputs, the parameters (µ and ů) of the probability density function (PDF). Therefore, as widely explained in the Manuscript, the number size distribution obtained by the experimental data of SEM XEDS microanalysis has been fitted to Log normal curve, as commonly performed in the literature on this issue (e.g. as in Mahowald et al., 2014)., and the PDF parameters have been obtained. Figure 4 shows the volume size

distributions of some minerals and of the different dust types, in the PM10 fraction, and are obtained directly from the experimental data of SEM XEDS microanalysis, as discussed in the Manuscript. Therefore size distributions in Figure 4 are not the result of a curve fitting.

p. 13357 L. 25. R: please rephrase

A: ñAn atmospheric radiative transfer code was employed, generally used in the remote sensing, to retrieve the optical and radiative dust properties.ò
This sentence has been changed in:
ñAn atmospheric radiative transfer code was employed to retrieve the optical and radiative dust properties.ò

p. 13358 L. 6. R: Dust particles are definitely not spherical. How much wrong can your result be? Can you give an estimate?

A: In this work, the assumption of particle sphericity has been adopted, due to the requirements of the 6SV code for radiative transfer modelling (as discussed in the Manuscript: ñThis code is able to retrieve optical properties of the aerosol and to model the atmospheric radiative field by using the aerosol microphysical properties, under the hypothesis of spherical and dry particles.ò).

This has been better clarified in the revised Manuscript, as follows:
ñPhysical size of particles was assumed as the diameter of the equivalent spherical cross sectional area (ESD) (Reid et al., 2003; Kandler et al., 2007; Choy l et al., 2007) measured by SEMò.
This sentence has been changed in:
ñIn this work, the assumption of particle sphericity has been adopted, due to the requirements of the 6SV code for radiative transfer modelling. Therefore, physical size of particles was assumed as the diameter of the equivalent spherical cross sectional area (ESD) (Reid et al., 2003; Kandler et al., 2007; Choy l et al., 2007) measured by SEM.ò

As explained in text, all parts of the study have been performed under the assumption of particle sphericity. As regards the simulation, an estimation of the accuracy can be performed in case of availability of measurements, or of ability of the model in simulating optical properties and radiative effect with non-spherical aerosol. This is not possible with the 6SV, as explained in [Kotchenova et al., 2008]: ñ*We also mention that all RT codes involved in this study used aerosol phase functions that were calculated on the basis of the Mie theory for homogeneous spheres. Such an assumption of sphericity is not valid for desert dust aerosols, which consist of mainly non-spherical particles with aspect ratios 1:5.*ò
The aspect ratio of the local dust used in the presented work is between 1:1 and 1:4 with a probability of 88% for a samples of 4800 particles. This value attests that the simulation of optical properties and the evaluation of RFE have been performed within the validity domain for the aerosol shape where the 6SV model meets the accuracy requirement of 1% for simulation studies [Kotchenova et al., 2008].

p. 1 13358 L. 21. R: Thus,

A: ñBy this way,ò has been changed with ñThus,ò

p. 13358 L. 26. R: why not using radiosondes from Rome's airport? or even reanalysis over the region? Should give an estimate of how wrong the result can be by doing this crude approximation.

A: ñConcerning meteorological parameters, the profiles of temperature, pressure and humidity were assumed by the 1976 U.S. Standard Atmosphere included in the 6SV code.ò

The radiosondes are useful if a comparison with radiative measurement is performed. In this work, the radiative effects have been simulated to evaluate the RFE of the two components of local dust. The variability of the meteorological parameters induces an error on RFE evaluation which is generally negligible with respect to the absolute values of RFE.
As reported in Garcia et al., 2008 ñ*The flux calculations are performed for multi-layered atmosphere with US standard atmosphere model for gaseous distributions and single fixed aerosol vertical distribution (exponential with aerosol height of 1 km). The deviations of these assumptions from the reality are also potential source of errors, although, our tests did not show any significant sensitivity of flux estimates to these assumptions. Differences less than 1 W/m2 due to different vertical profiles were observed on the downward solar flux at the bottom of the atmosphere.*ò

p. 13359 L. 5. R: higher than what? you did not mention other AOD value before.

A: ñIn this study, however, an higher value of aerosol optical thickness, Ű550 = 0.7, was chosen....ò The adjective has been corrected as follows:
ñIn this study, however, an high value of aerosol optical thickness, Ű550 = 0.7, was chosen..ò.

p. 13359 L. 8. R: This is only true if other aerosol sources in the region always give contributions of AOD << 0.7. Please cite the previous studies how showed that. or use AERONET data from Rome or L'Aquila. In this case you could even get an inverted size distribution and evaluate if the strong dust episodes indeed happen or not in your region.

A: The authors have previously explained that the radiative simulation are referred to one component of the local dust, as yet discussed in the reply provided concerning p. 13348 L. 25, and any comparison to radiative measurements or AERONET products are not useful for the purposes of this work.

p. 13359 L. 10. R: chosen from what? Where? since you got a refraction index form the literature and are running a Mie code you should calculate g and w

A: ñAmong optical properties, the single-scattering albedo and the asymmetry parameter were chosen, as they are crucial to perform analysis of the aerosol contribution on the radiative field (Dubovik et al., 2002; Kassianov et al., 2007).ò
The sentence has been rewritten as:
ñAmong simulated optical properties, the single-scattering albedo and the asymmetry parameter were presented, as they are crucial to perform analysis of the aerosol contribution on the radiative field (Dubovik et al., 2002; Kassianov et al., 2007).ò

The Mie theory is implemented in 6SV model and its runs *simulate* the optical properties, including single-scattering albedo and asymmetry parameter, and the radiative quantities describing the radiative field in the Earth/Atmosphere coupled system.

p. 13360 L. 5. R: Legend of Table 1 should properly explain the units. What is % rsd? What is ±- prop.err.? Why the consistency is not shown for travertine?

A: The editorial rules of ACP indicate that extended legends should be avoided. Anyway the units in Table 1 have been described in the footnotes at bottom of Table 1. Consistency of the microanalysis on extended fields of the sample with results by EDXRF is not shown for travertine, as field acquisitions by SEM XEDS have been not performed on this sample, given the basically constant calcite concentration in the matrix of this sample.

p. 13360 L. 11. R: Why do you say XEDS is less reliable than EDXRF? To assess that you should compare both to the same PM standard from NIST.

A: Arguments concerning this issue have been extensively discussed in the reply to General concerns #1.

p. 13361 L. 4. R: Did you use a NIST standard or not? Line 8, last page = you say ñdust sampleò.

A: Arguments concerning this issue have been extensively discussed in the reply to General concerns #1. Particularly, please consider the following part of the reply to General concerns #1: ñit should be considered that quantification methods properly targeted on the SEM XEDS microanalysis of individual particles from environmental matrices does not exist, as discussed in the Manuscript (Section 2.3), and standard materials of environmental particulate matter properly dedicated to the quantification of the elemental composition of individual particles (relating to individual particles from environmental matrices) are not available. For this reason, the authors applied an internal standard approach to achieve the goal of quantification of particle elemental composition, which is an unavoidable step in the analytical structure of this study, and assessed the reliability of this approach (and of the procedure of particle allocation to mineral classes) by comparison with the quantitative results of elemental composition obtained by EDXRF on the bulk PM10 dust samples.ò

p. 1 13361 L. 18. R: PCA cannot be used in your case because itc allows negative concentrations (or mass). PMF (positive matrix factorization) is the reference method in this case.

A: In this work the PCA is employed to discuss results of the elemental ratios obtained by SEM XEDS microanalysis of individual dust particles; no limitation exists, to the authorôs knowledge, in applying the PCA to this type of data. This issue has been yet discussed in the reply to General concerns # 2.

p. 13362 L.7. R: What did you do in order not to get any negative values in figure 2? If you modified the standard PCA technique you should explain what was doneé

A: Please refer to reply to the previous comment and to General concerns # 2.

p. 13363 L. 16. R: I donôt see how this inference can be made, since you did not measure atmospheric aerosol particles. For the lab. Method you used, you should already know if weathering is most important.

A: In the discussion related to this point of the manuscript, the term óweatheringô is used to indicate processes of rock alteration, and not weathering from atmospheric factors. The suitability of using this term in this case is linked both to the fact that we are discussing the possible lithological processes which are responsible of the mineralogical composition of the PM10 dust samples obtained ñat sourceò from the outcropped rocks (or topsoil, depending on the samples), as clarified and discussed in the previous comments, and to the fact that this term is commonly used in the geochemistry research field to indicate rock alteration processes.
The sentence related to this comment has been rephrased as follows:
ñThe mineralogical composition of the silicate component in marlstones and siliciclastics dust is strictly related to the originating materials. Rock-forming processes (erosion, fluvial and marine transport, sedimentation) support, in this case, the presence in the PM10 fraction, as detected by XRD, of stable silicates (plagioclase and quartz), the reduced presence of inosilicates and the presence of alteration by-products, such as phyllosilicates. Different processes must be considered in volcanic rocks, which explain the mineralogical composition of silicates observed in the PM10 resuspended from this geological material; specifically, crystallization is the main responsible process, in this case. Thus, the presence of most minerals observed in the PM10 from volcanic rocks is coherent with the magmatological framework of Central Italy. Differently from the above considerations, however, the association kaolinite ï quartz, observed by SEM XEDS microanalysis in this PM10 dust type, has to be ascribed to rock alteration (weathering). In this case quartz is thus the product (with kaolinite) of the hydrolysis reaction of feldspars (Jackson et al., 2010), and not a crystallization-derived phase.ò

p.1 13363 L. 19. R: Presence where?

A: Please refer to reply to previous comment.

p. 13368 L. 17. R: Isnôt the lab method to produce these particles much more important?

A: Please refer to reply to General concerns #3, where this issue has been extensively discussed.

p. 13369 L. 19. R: Why is this figure so much different from fig. 4? In Fig. 4 the largest size are > 5 µm, but in figure 5 it is < 2 µm. The max concentration is also different. The data points should include the uncertainties as well (and those should be used in the fit). Moreover, as you donôt see the decrease for large radius, the uncertainty associated with the fitted std will be very large and should be discussed. Last, quality quality of this figure does not fit publication standards. Are you should you included the right figure?

A: Figure 5 shows the probability density function (PDF) obtained from the fitting to Log normal curve of the number size distributions experimentally obtained by SEM XEDS microanalysis data, which is reported versus the physical radius of particles, while Figure 4 shows volume size distributions experimentally obtained by the same SEM XEDS dataset, which are reported versus the aerodynamic diameter of particles, therefore these two figures are necessarily different.
The whole procedure to obtain results of figures 4 and 5 is described in details in the Manuscript.

The uncertainty of each bin was estimated associating a Poisson error to the bin weight (Liley, 1992), that is calculating the square root of the total counts of particles observed in each size range. Figure 5 has been replaced in the revised Manuscript, including uncertainties. Furthermore, as the PM10 samples of this study have been obtained by sampling with a PM10 sampling head compliant with EN12341 standard (as reported in the paper by Pietrodangelo et al., 2013, cited in Section 2.1 of the Manuscript), particles have aerodynamic diameter below 10µm, which is coherent with the fact that in the PDF data related to particle radii larger than 3 µm are not present (considering an average particle density of 2.71). Furthermore, our results concerning the fitted PDFs are in line with results reported by Mahowald et al. (2014), which review the data reported by many studies dealing with size distribution of mineral dust samples obtained by chamber resuspension or by field sampling at source. An extract from this paper, reporting details on this issue, is reported in the reply to General concerns # 3.

Following the Reviewerôs suggestion, the following sentence has been added in the revised Manuscript (Section 3.5.1):
ñResults of fitting are in line with findings discussed by Mahowald et al. (2014). ñ

Finally the quality of figure 5 has been checked by the editorial office of Copernicus during the first submission process, and any problems have been evidenced on it; indeed, it was provided as .eps file.

p. 13370, values of r and ů R: What are the uncertainties associated with these values? What are the units?

A: Uncertainties and units of r and ů values have been added in the revised Manuscript.

p. 13370 L. 12. R: how can you be sure that these dust measurements correspond to the optical properties of your samples? what are the associated uncertainties with the following estimates?

A: ñThe other microphysical property required for 6SV run is the refractive index. In Fig. 6 the real (n) and imaginary (k) part of the refractive index have been interpolated at the 6SV twenty wavelengths (350; 400; 412; 443; 470; 488; 515; 550; 590; 633; 670; 694; 760; 860; 1240; 1536; 1650; 1950; 2250; 3750 nm), following the spectral data of water-insoluble (Kokhanovsky, 2008; WCP-112, 1986) and calcite-rich dust (Ghosh, 1999) refractive index, respectively related to volcanics and travertine.ò

In the 6SV, the Mie theory is used to estimate optical properties of an aerosol type on the basis of its microphysical properties (i.e., size distribution and refractive index). The authors have yet discussed, in the previous replies, the need of adopting from literature values of the real and imaginary parts of the refractive index in the spectral range within which the 6SV performs the radiative transfer modelling. As experimental measurements of the optical properties of dust types of this study are not available, it is not possible to give an estimation of the uncertainties of the 6SV modelling results. It has to be also taken into account that the 6SV simply apply the Mie Theory with the required assumptions, particularly referring to the assumption of particle sphericity.

p. 13370 L. 26. R: these.

A: ñthisò should be used, in this case, as it is referred to ñdust typeò.

p. 13371 L. 1. R: rephrase

A: ñThe radiative modeling has been focused on the downward component of the radiative impact at BOA due to the volcanics and travertine dust in Rome area.ò
This sentence has been rephrased in: ñThe radiative modeling has been focused on the downward component of the radiative impact at BOA influenced by the volcanics or the travertine dust in Rome area.ò

p. 13371 L. 18. R: this is not what is shown in Fig.9. It shows that both give the same BOA irradiance. To say they don't affect direct radiation you would need to simulate the same atmosphere with any dust at all.

A: ñBoth volcanic and travertine dusts leave the direct component unchanged, while the diffuse component depends strongly on the mineral composition.ò
This sentence has been rephrased in:
ñDirect components calculated in presence of volcanic-only and of travertine-only dusts shows negligible differences, while the diffuse component depends strongly on the mineral composition.ò

The authors have previously explained that the simulations have been performed by using each one of the two components, separately. The direct component of the BOA irradiance is the same whereas the diffuse component depends on the dust component used for the simulation as reported in Fig. 9.

p. 13372 L. 26. R: You could have concluded that without any RT simulation... Just the large difference in your ADHOC index of refraction for the two species were enough to justify it.

A: The following sentence has been deleted in the revised Manuscript: ñNevertheless, the charge **(???)** of differences existing in the Rome local mineral dust composition on the variability of optical and radiative properties of the airborne aerosol appears as a key issue, to be further considered in the radiative balance analysis.ò.

The real and imaginary parts of the complex refractive index can justify, but the RFE cannot be evaluated without a RT model. Furthermore, the RT models are a powerful and necessary tool recognized for accurate simulation of the radiative field and widely applied to the Earth Observation data.

List of relevant changes in the revised manuscript

Title: the original title has been revised in: ‘Composition, size distribution, optical properties and radiative effects of laboratory resuspended PM10 from geological dust of Rome area, by electron microscopy and radiative transfer modelling’.

Abstract:

- first part of the abstract has been revised in: ‘In this work, new information has been gained on the laboratory resuspended PM10 fraction from geological topsoil and outcropped rocks representative of Rome area, Latium. Mineral composition, size distribution, optical properties and the surface radiative forcing efficiency (RFE) of dust types representing the compositional end-members of this geological area have been addressed. A multi-disciplinary approach was used, based on chamber resuspension of raw materials and PM10 sampling, to simulate field sampling at dust source, scanning electron microscopy / X-ray energy-dispersive microanalysis (SEM XEDS) of individual mineral particles, X-ray diffraction (XRD) analysis of bulk dust samples, building of number and volume size distribution (SD) from microanalysis data of mineral particles and fitting to Log-normal curve, and radiative transfer modelling (RTM) to retrieve optical properties and radiative effects of the compositional end-member dust samples’.
- A new sentence has been added at the end: ‘The RFE (293 W/m2 for volcanics and 139 W/m2 for travertine, at 50° solar zenith angle) shows that volcanics dust produces a stronger cooling effect at surface than travertine, as expected for more absorbing aerosols’.

Introduction:

- first sentence has been revised in (a new reference has been added coherently): ‘Airborne geological dust sourced from topsoil and surface rocks critically contribute to the total mass, composition, microphysical and optical properties of the atmospheric aerosol in continental regions, and largely impacts different Earth’s compartments by transport and deposition (Scheuvens and Kandler, 2014)’.
- a new part has been added to discuss Figures 2S and 3S (new, added to the Supplementary materials): ‘Consequently, the resuspension of mineral dust from local lithological domains contributes notably to the ambient PM10 of Rome area. This is shown in Figures 2S and 3S for the Villa Ada site (Rome, urban background) and the Montelibretti EMEP site (Rome outskirts, rural background), respectively. Considering the 2005 – 2011 period, among days which show a dominant (over 50% of total PM10 mass) crustal contribution to the ambient PM10 composition at these sites, desert dust intrusions at-ground (DD-days) account for 60% at Montelibretti and 30% at Villa Ada, while the remaining days are reasonably affected by local crustal contributions, given the background character of the considered sites (LD-days). Interestingly, among the above described days, the mass concentration of the crustal matter on LD-days is in many cases comparable with that observed on DD-days’.

Section 2.1:

- the sampling criteria have been revised in:

óSampling areas of about 4 km^2 were selected within each local geodynamics domain; a number of dust collection points was identified, within each area, to obtain sub-samples of raw material, from which the final samples were obtained. The number of sampling areas varies within each domain, depending on the geographical extension and the geological complexity of the domainô.

- a new sentence on the suitability of chamber resuspension approach to the goals of this study has been added (new references have been added coherently):

ó*It is worth noting that, among laboratory methods of dust generation or resuspension from bulk materials, fluidization by mechanical ventilation in a resuspension chamber is widely acknowledged, either for not affecting both the complete resuspension potential of the source material and the original size distribution of the resuspended particles in the material itself, and for simulating the resuspension of dust previously deposited at a site (Gill et al., 2006 and references therein). By this approach, good approximation of the field sampling at a dust source can be achieved, making it suitablefor studies on the mineralogical and microphysical characterization of mineral dust (Gill et al., 2006 and references therein; Feng et al., 2011; Aimar et al., 2012; Dobrzhinsky et al, 2012).*ô

<u>Section 2.2</u>: a new sentence has been added concerning the calibration of the SEM XEDS instrument:

ó*Instrumental calibration of the magnification and of the XEDS spectrometer gain are routinely performed on the basis of the US EPA Guideline for SEM EDX microanalysis of particulate matter samples (Willis et al., 2002)*ô.

<u>Section 2.3</u>:

- the title has been revised in: ó*Quantification of individual particles XEDS spectra and procedure of particle allocation to mineral classes*ô;

- the fully detailed description of the internal standard approach to semi-quantification of the individual particle elemental composition has been moved to Appendix I (new), in the Supplementary materials.

<u>Section 2.4</u>: a new sentence has been added at the beginning of this section:

ó*In this work, the assumption of particle sphericity has been adopted, due to the requirements of the 6SV code for radiative transfer modelling.*ô

<u>Section 2.4.1</u>: a new sentence has been added concerning the uncertainties of the fit to Log-normal curve: ó*The uncertainty of each bin was estimated associating a Poisson error to the bin weight (Liley, 1992), that is calculating the square root of the total counts of particles observed in each size range.*ô

<u>Section 2.5:</u>

- a new sentence has been added concerning adopting refractive index data from literature:

ó*This choice was driven by the fact that the 6SV code requires as input the spectral trend of the real and imaginary parts of r.i., and these measurements were not available from our laboratory.*ô

- a new sentence has been added to describe the radiative forcing efficiency (RFE) at BOA, newly introduced in the revised version of the manuscript to describe the radiative effects of the volcanics and travertine dusts independently on the aerosol loading (new references have been added coherently):

ôIn order to evaluate the direct radiative effect at the surface of the two local dust components, the radiative forcing efficiency (RFE) at BOA has been considered. In a recent modelling study, Gomez-Amo et al. (2011) derives the RFE by using a radiative transfer code. In this study, the RFE has been computed for each component by the difference between the BOA flux simulated by 6SV code in case of atmosphere with and without the dust component in the 250 - 4000 nm spectral domain and normalized with respect to the AOT at 550 nm (Garcia et al., 2008). The comparison between the RFE of volcanic and travertine allows to analyse the dependence of surface forcing from aerosol types (microphysical properties) and SSA independently from the aerosol loading (di Sarra, 2008, 2013; Di Biagio et al., 2010)ô.

<u>Section 3.3</u>: the part concerning pedogenic and alteration processes of rock / topsoil to which the mineralogical composition of the lithogenic PM_{10} can be related has been revised in:

ôThe mineralogical composition of the silicate component in marlstones and siliciclastics dust is strictly related to the originating materials. Rock-forming processes (erosion, fluvial and marine transport, sedimentation) support, in this case, the presence in the PM_{10} fraction, as detected by XRD, of stable silicates (plagioclase and quartz), the reduced presence of inosilicates and the presence of alteration by-products, such as phyllosilicates. Different processes must be considered in volcanic rocks, which explain the mineralogical composition of silicates observed in the PM_{10} resuspended from this geological material; specifically, crystallization is the main responsible process, in this case. Thus, the presence of most minerals observed in the PM_{10} from volcanic rocks is coherent with the magmatological framework of Central Italy. Differently from the above considerations, however, the association kaolinite ï quartz, observed by SEM XEDS microanalysis in this PM_{10} dust type, has to be ascribed to rock alteration (weathering). In this case quartz is thus the product (with kaolinite) of the hydrolysis reaction of feldspars (Jackson et al., 2010), and not a crystallization-derived phase.ô

<u>Section 3.4.1</u>: a new part has been added concerning the obtained mineralogical composition in comparison with other studies (new references have been added coherently):

ôWith respect to the mineralogical profiles of PM_{10} dust from sources located in North Africa (N.A.) and Saudi Arabia (S.A.) (Ganor et al., 2009), the dust samples of this study show the following differences: 1) large variability in terms of calcite content (up to 90% in travertine), compared to PM_{10} from N.A. and S.A. (20-30%); 2) large variability in terms of tectosilicates (up to 20% in volcanics) and clay minerals (up to 57% in volcanics) compared to PM_{10} from N.A. and S.A. (1-3% 30-40% respectively); amount of quartz comparable to that in PM_{10} from N.A. and S.A. (2-4%) in the case of the siliciclastic PM_{10}, but significatively different in travertine (undetectable) and in volcanics (10%). Moreover, the presence of inosilicates is not reported for the PM_{10} from N.A. and S.A., while the latter show the presence of gypsum, not observed in the PM_{10} dust samples of this studyô.

Section 3.5.1: uncertainties and units have been added to the reported parameters of the Log-normal curve of volcanics and travertine dusts

Section 3.5.3: a new part has been added at the end of this section to discuss results of the RFE calculations:

óThe evaluation of the radiative budget at surface of the local mineral dust in Rome area has been performed computing the RFE. The RFE is calculated by simulating the total BOA downward flux with the local dust component in three conditions of AOT at 550 nm (0.2; 0.5; 0.7), to estimate the uncertainty on the simulated RFE. The results highlight the stronger cooling effect at the surface in case of volcanic (-293 ± 17 W/m2) respect to travertine (-139 ± 7 W/m2) with uncertainties lower than 5%. The aerosol radiative behaviour follow the general trend explained in Gomez-Amo et al., (2011), that is aerosols with high SSA (low absorption, travertine in case) produce a decrease in the absolute value of RFE, with respect to aerosols t characterized by high absorption, like the volcanicsô.

Conclusions: a new part has been added to address conclusions about the RFE of volcanics and travertine dusts:

óThe radiative effects of the two components in the 350 - 3750 nm spectral domain have been evaluated by the RFE; results show higher efficiency of volcanic (-293 ± 17 W/m2) in surface cooling effect, with respect to travertine (-139 ± 7 W/m2), as expected for aerosol with SSA smaller than 1 (Di Biagio et al., 2010), that is the volcanics dust in this case.ô

Acknowledgements: a new sentence has been added:

óFinally, we are grateful to Alcide di Sarra (ENEA, Laboratory for Earth Observations and Analyses) for helpful comments and suggestions that greatly improved the radiative transfer issues in the manuscript.ô

References: new references have been added, and some have been deleted, as indicated in the marked version of the revised manuscript reported below.

Table 1: units have been detailed in the footnotes at bottom of the table, as indicated in the marked version of the revised manuscript reported below.

Figure 5: this figure has been replaced by the same figure, where uncertainties have been added; figure caption has been revised consequently.

Supplementary materials:

- Appendix I (new) has been added:

-title: óInternal standard approach to quantification of particle elemental composition from SEM XEDS microanalysisô;

- text: the same text originally included in the second part of Section 2.3 has been deleted from Sect. 2.3 and reported as Appendix I.

Figure 2S and 3S (new): these figures (and related captions) have been added to support the new part included in the revised Introduction.

Composition, size distribution, optical properties and radiative effects of laboratory resuspended PM_{10} from geological dust of Rome area,~~re-suspended local mineral dust of Rome area~~ by electron microscopy~~individual-particle microanalysis~~ and radiative transfer modelling

A. Pietrodangelo,[1] R. Salzano,[1] C. Bassani,[1] S. Pareti,[1] and C. Perrino[1]

(1){ Institute of Atmospheric Pollution Research, National Research Council, Italy }

Correspondence to: A. Pietrodangelo (pietrodangelo@iia.cnr.it)

Abstract

In this work, new information has been gained on the laboratory resuspended PM_{10} fraction from geological topsoil and outcropped rocks representative of Rome area, Latium.

Mineral composition, size distribution, optical properties and the surface radiative forcing efficiency (RFE) of dust types representing the compositional end-members of this geological area have been addressed.~~New information on the PM_{10} mineral dust from site-specific (Rome area, Latium) outcropped rocks, and on the microphysics, optical properties and radiative effects of mineral dust at local level were gained in this work.~~ A multi-disciplinary approach was used, based on chamber resuspension of raw materials and PM_{10} sampling, to simulate field sampling at dust source,~~on individual particle~~ scanning electron microscopy ~~with~~ / X-ray energy-dispersive microanalysis (SEM XEDS)~~,~~ of individual mineral particles, X-ray diffraction (XRD) analysis of bulk dust samples, building of number and volume size distribution (SD) from microanalysis data of mineral particles and fitting to Log-normal curve, and radiative transfer modelling (RTM) to retrieve optical properties and radiative effects of the compositional end-member dust samples. The mineralogical composition of Rome lithogenic PM_{10} varies between an end-member dominated by silicate minerals (from volcanic lithotypes), and one ~~exclusively~~ mostly composed of calcite (from travertine or limestones).

~~The first is obtained from volcanic lithotypes, the second from travertine or limestones;~~ L~~l~~ithogenic PM_{10} with intermediate composition derives mainly from siliciclastic rocks or marlstones~~ of Rome area~~. Size and mineral species of PM_{10} particles of silicate-dominated dust types are tuned mainly by rock weathering and, to lesser extent, by debris formation or crystallization; chemical precipitation of $CaCO_3$ plays a major role in calcite-dominated types. These differences ~~are evidenced by~~reflect in the diversity of volume distributions, either within dust types, or mineral species. ~~Further d~~Differences are also observed between volume distributions of calcite from travertine (natural source; SD unimodal at 5 µm a.d.) and from road dust (anthropic source; SD bimodal at 3.8 and 1.8 µm a.d~~), specifically on the width, shape and enrichment of the fine fraction (unimodal at 5 µm a.d. for travertine, bimodal at 3.8 and 1.8 µm a.d. for road dust)~~. ~~Log-normal probability density functions~~SD ~~of~~ The volcanics and travertine dusts affect differently the single scattering albedo (SSA) and the asymmetry

parameter (g) in the VISible and Near Infrared (NIR) regions~~, depending also on the absorbing/non-absorbing character of volcanics and travertine, respectively~~.

The downward component of the Bottom Of Atmosphere (BOA) solar irradiance simulated by RTM for ~~a volcanics-rich or travertine-rich~~ an atmosphere where only volcanics, or only travertine dust, composes the aerosol, shows that volcanics contribution to the solar irradiance differs significantly from that of travertine in the NIR region, while similar contributions are modelled in the VIS. The RFE (293 W/m^2 for volcanics and 139 W/m^2 for travertine, at 50° solar zenith angle) shows that ~~local~~ volcanics dust produces a stronger cooling effect at surface ~~if the dust is composed by volcanic respect to by~~than travertine, as expected for more absorbing aerosols.

1 Introduction

Airborne geological dust sourced from topsoil and surface rocks ~~from topsoil and surface rocks represents a~~ critically ~~contribution~~ contribute to the total mass, composition, microphysical and optical properties of the atmospheric aerosol in continental regions, and largely impacts different Earthôs compartments by transport and deposition (Scheuvens and Kandler, 2014). ~~The occurrence of lithogenic dust in the atmosphere implies that significant amounts of biological debris, complex organic molecules (i.e. humic-like substances), water and mineral particles may enter the composition of the airborne particulate matter (PM) (Hsu and Divita, 2009; Simon et al., 2010)~~. Crustal particles commonly constitute the major mass fraction of the re-suspended lithogenic materials and influence significantly both the PM mass concentration at ground (Perrino et al., 2009; Viana et al., 2014) and the mineral composition. The latter varies mostly depending both on the rock types outcropping in the source region (Dürr et al., 2005; Journet et al., 2014) and, consequently, on the crystallization, sedimentation and weathering processes tuning the particle size and shape (Claquin et al., 1999). This has been observed for mineral dust of African desert regions (Caquineau et al., 2002; Evans et al., 2004; Stuut et al., 2009; Scheuvens et al., 2013; Formenti et al., 2014) and

of arid areas in other regions (Kim et al., 2006; Jeong, 2008; Moreno et al., 2009; Agnihotri et al., 2013; Rashki et al., 2013). Either microphysical (size distribution and complex refractive index) and optical properties of airborne lithogenic dust vary as a consequence of the mineralogical composition (Sokolik and Toon, 1999; Reid et al., 2003; Hansell et al., 2011; Wagner et al., 2012; Di Biagio et al., 2014; Mahowald et al., 2014; Smith and Grainger, 2014). When at a certain site intrusions of lithogenic dust at ground occur, like desert dust, the overall properties of the PM may be altered, compared to periods when this contribution is negligible (Meloni et al., 2006; Choobari et al., 2014). This also affects the impact of airborne aerosol on the energy balance of the Earth ï solar system. Airborne lithogenic dust plays a role both in the direct mechanisms (light scattering and absorption) and in the indirect mechanisms (~~warming or cooling of the atmosphere~~cloud-aerosol interactions) which tune the Earthôs radiative budget (Sokolik et al., 2001; Choobari et al., 2014). While indirect effects depend on the heterogeneous chemistry occurring at particles surface (Levin et al., 1996; Buseck and Pósfai, 1999; Sokolik et al., 2001; Krueger at al., 2004; Kandler et al., 2007), the light scattering and absorption are mostly controlled by the mineralogical composition, shape features and microphysical properties of geological particles ((DôAlmeida, 1987; Kalashnikova and Sokolik, 2002 and 2004; Kokhanovsky, 2008; Hansell et al., 2011).

Most studies facing this issue relate to desert dust from Sahara and Sahel regions (Kandler et al., 2007 and 2009; Müller et al., 2009; Papayannis et al., 2012; Wagner et al., 2012; Di Biagio et al., 2014). Nevertheless, knowledge gaps still exist on this issue (Rodríguez et al., 2012), due to the site-related large variability of dust mineralogical features (elemental and mineral composition, crystalline structure, shape, microphysical and optical properties).

Also, only few of the published studies characterize the re-suspended geological dust of non-African regions (Falkovich et al., 2001; Peng and Effler, 2007; Rocha-Lima et al., 2014). Large areas of Italy, especially those closer to the Mediterranean Basin, are affected by dryness, heavy anthropic impact (urbanization, farming, quarry activities, etc.), erosion and poor vegetation cover, leading to increased desertification risk. The National Atlas of areas under risk of desertification of Italy reports, for instance, that the yearly average of dry soil days in the region of Latium ranges 64 ÷ 110 (Costantini et al., 2007 and 2009). In Fig. 1S this is showed for the area of study of this work; the highest number of dry soil days (86 ÷ 110) is found in the northern zone of the study area (Geoportale Nazionale, 2011). Latium is also ~~affected by high rain aggressiveness, within the scale of FFAO index, and is~~

characterised by a large surface where poorly-developed soils and debris deposits are present, which are easily affected by massive erosion.

~~Considering also the high anthropic impact on the Latium territory, it has to be expected that t~~Consequently, the ~~re suspension~~resuspension of mineral dust from local lithological domains ~~is non negligible~~contributes notably to the ambient PM_{10} of ~~in this region~~Rome area. This is shown in Figures 2S and 3S for the Villa Ada site (Rome, urban background) and the Montelibretti EMEP site (Rome outskirts, rural background), respectively. Considering the 2005 ï 2011 period, among days which show a dominant (over 50% of total PM_{10} mass) crustal contribution to the ambient PM_{10} composition at these sites, desert dust intrusions at-ground (DD-days) account for 60% at Montelibretti and 30% at Villa Ada, while the remaining days are reasonably affected by local crustal contributions, given the background character of the considered sites (LD-days). Interestingly, among the above described days, the mass concentration of the crustal matter on LD-days is in many cases comparable with that observed on DD-days. Within this picture, main goals of this work were: to study the relationships between the local outcropped rocks (or topsoil) and the ~~airborne~~ dust particles in the PM_{10} ~~dust particles~~ sourced from these rocks, and to gain knowledge about the ~~influence of local mineral dust on the airborne PM in Rome, in terms of~~ microphysical and optical properties of the mineral PM_{10} at geological dust source, and on ~~by modelling~~ the downward radiative flux at BOA (Bottom Of Atmosphere) ~~relating to the presence of local mineral dust~~related to an atmosphere where the only aerosol component is the PM_{10} dust, in order to define the radiative effects which are due to the local mineral dust only~~.~~ In a previous study, we determined elemental source profiles of the PM_{10} fraction of local mineral dust (Pietrodangelo et al., 2013). In this work, the PM_{10} fraction of the same samples was characterized with respect to the above goals. To investigate relationships among these different aspects, a multi-faceted analysis was performed, on the basis of the following approaches: chamber resuspension of raw materials and PM_{10} sampling, to simulate field sampling at dust source, scanning electron microscopy / X-ray energy-dispersive microanalysis (SEM XEDS) of individual mineral particles, X-ray diffraction (XRD) analysis of bulk dust samples, number and volume size distribution (SD) building from microanalysis data of mineral particles and fitting to Log-normal curve, and radiative transfer modelling (RTM) to retrieve optical properties and radiative effects. ~~individual particle scanning electron microscopy combined with X ray energy dispersive~~

~~microanalysis (SEM XEDS), bulk mineralogical analysis by X-ray diffraction (XRD), parameterization of the size distribution to log-normal function, and radiative transfer modelling (RTM).~~ Results from experimental and modelling analysis are discussed for their consistency with both the lithological nature of major local dust sources and the microphysical properties of the mineral dust samples.

2 Approach and methodology

2.1 Study area, dust collection and sample treatment

Mineral dust was collected from topsoil and debris of rural areas surrounding the city of Rome within a perimeter of 50 km radius. On the basis of criteria established after geological analysis of the Latium region, the following geodynamics domains were considered: the volcanic complexes, the marine (limestones, marlstones and sandstones) deposits, the siliciclastic series (mainly flysch) and the quaternary deposits (mainly travertines).~~Collection~~ Sampling areas of about 4 km^2 were selected within each local geodynamics domain; a number of dust collection points was identified, within each area, to obtain sub-samples of raw material, from which the final samples were obtained. The number of sampling areas varies within each domain, depending on the geographical extension and the geological complexity of the domain. ~~on the basis of criteria established after geological analysis of the Latium region, within main local geodynamics domains, namely: the volcanic complexes, the marine (limestones, marlstones and sandstones) deposits, the siliciclastic series (mainly flysch) and the quaternary deposits (mainly travertines).~~ Furthermore, paved road dust was collected by brushing the surface of different roads within the volcanic and the travertine domains. PM_{10} dust was laboratory re-suspended from the bulk rocks samples, and from road dust, by a ~~re-suspension~~resuspension chamber, and collected by low-volume sampling on polycarbonate membranes for SEM XEDS microanalysis. It is worth noting that, among laboratory methods of dust generation or resuspension from bulk materials, fluidization by mechanical ventilation in a resuspension chamber is widely acknowledged, either for not affecting both the complete resuspension potential of the source material and the original size distribution of the resuspended particles in the material itself, and for simulating the resuspension of dust previously deposited at a site (Gill et al., 2006 and references therein). By this approach, good approximation of the field sampling at a dust source can be achieved,

making it suitable; therefore, it is commonly used in the research field offor studies on the mineralogical and microphysical characterization of mineral dust (Gill et al., 2006 and references therein; Feng et al., 2011; Aimar et al., 2012; Dobrzhinsky et al, 2012). The whole geological siting criteria, dust sampling strategy, laboratory treatment details and elemental profiles of the re-suspended dust types, are fully described in Pietrodangelo et al. (2013). In that paper we discussed how, under the perspective of mineral composition, the volcanics (silicate-dominated rocks) and the travertine (calcite-dominated rocks) can be considered as reference compositional end-members of the overall outcropping lithotypes in the Latium region (Cosentino et al., 2009), while the sedimentary domains (marine deposits and siliciclastic series) represent intermediate compositional terms. Therefore, for the scopes of this work the complete procedure of dust characterization (elemental and mineral composition, size distribution, optical properties and radiative downward flux) described in the following sections was applied only to the volcanics and travertine dust.

2.2 Individual particle microanalysis

An environmental scanning electron microscope Philips XL30 ESEM (FEI Company, tungsten filament) equipped with an energy dispersive spectrometer for x-ray microanalysis (EDAX/AMETEK Inc.,USA) was used for individual particle characterisation of the PM_{10} dust. Instrumental calibration of the magnification and of the XEDS spectrometer gain are routinely performed on the basis of the US EPA Guideline for SEM EDX microanalysis of particulate matter samples (Willis et al., 2002). A small portion of sample (about 8% of total filter area) was cut in the centre of polycarbonate membranes, fixed to aluminium stubs by self-adhesive carbon discs (TAAB, 12 mm diam.) and coated with an ultra-thin carbon layer by a vacuum evaporator (108 Carbon A, Cressington, Scientific Instruments Ltd., U.K.). SEM XEDS acquisitions were performed under high vacuum (10^{-6} hPa) at 20 keV accelerating voltage, allowing the K-line excitation of elements with atomic number Z Ò27 (Co, KŬ6.923 keV). Micrographs were acquired by secondary electron detector (SED) at magnification, working distance (WD), tilt angle and spot size conditions properly adjusted on a case-sensitive scale to optimize image resolution. The microanalysis was performed at WD 10 mm (take-off angle 35° relative to the specimen plane) on field areas of 1290 ï 5200 εm^2 (magnitude x 6000-3000) spread on the overall specimen surface; between 700 and 1000 particles were analysed per sample.

The Particle/phase analysis v.3.3 package (EDAX Inc., 2000) was used for the automated individual particle microanalysis; threshold of the digitalised object area to be analysed was set at 80%. Since a great number of individual particles was analysed, short live times (20ï 30 s) were imposed to XEDS spectra acquisition. Each field of microanalysis was manually selected prior to launching the automated scanning of particles. This choice allows a field-specific tuning of the grey scale, in order to minimize brightness *artifacts* in the automated identification of particles. Amplification time and spot size were adjusted to ensure dead time around 30% and total counts rate above 500 cps. In addition to automated microanalysis, manual acquisitions were carried out, ~~either~~ both on field areas and on individual particles, by using the EDAX control v. 3.3 package (EDAX Inc., 2000). About 20 to 30 field areas were selected from the different dust samples to perform manual acquisitions. These have been run in triplicate on each field (live time 10 ï 20 s), to assess the repeatability of the microanalysis.

Further, XEDS spectra acquired from areas included in these fields were quantified by the conventional standard-based quantification procedure of bulk materials, to assess consistency with results previously obtained by ED-XRF analysis (Pietrodangelo et al., 2013).

Manual microanalysis of 15 to 30 individual particles per-sample was also performed, and high resolution micrographs of these particles were stored. Magnification above 6000x and longer live times (30 - 60 s) were employed, so that resulting XEDS spectra have total counts rate ranging 5000-10000 cps. These data were used both to assess the accuracy of microanalysis with respect to different mineral particles (Table 1), and to perform the quantification of individual-particle XEDS spectra by an internal standard approach, as further discussed in Sect. 2.3 and 3.1.1.

2.3 Quantification of individual particle XEDS spectra and ~~apportionment~~procedure of particle allocation to mineral classes

A large data set of XEDS spectra and size (Feret diameters, area, aspect ratio, roundness) of individual dust particles was stored. To ~~apportion~~ allocate dust particles into main mineral classes of our dust samples, an ad-hoc procedure has been adopted.

First, the bulk mineral composition of dust samples was determined by x-ray diffraction (XRD), to identify major minerals in the dust samples. Then, XEDS spectra of individual particles were semi-quantified and matched to spectra and to elemental composition of

reference pure minerals expected after XRD analysis. Results of matching were used to apportion individual particles into main mineral classes. Details are described below and~~below~~in Appendix 1 of supplementary materials.

The mineralogical characterization of dust samples has been carried out on the 50 µm sieved dust fraction, by an automatic diffractometer Scintag X1, equipped with a Si(Li) detector using a Cu KŬtarget, under the following conditions: Ni-filtered radiation, step-scan modality (2° step = 0.02°), acquisition time of 10 s, operating at 45 kV and 40 mA. Quantification of minerals has been obtained according to procedures defined by Moore & Reynolds (1997).

A random orientation of particles was obtained by pressing 0.5 g of the 50 ɛm sieved materials with 5 atm for 10 s. Quantitative determinations were obtained by using appropriated standards and elaborating spectra as indicated in Giampaolo and Lo Mastro (2000). From XRD results and on the basis of previous geological analysis of the area, mineral species to which individual dust particles have to be apportioned were identified.

Allocation of individual dust particles analyzed by SEM XEDS to mineral classes can be carried out by matching XEDS spectra of particles to those of pure minerals.

However, XEDS spectra of some minerals can be not available; in this case, allocation can be performed by matching the quantified elemental composition of particles with that of pure minerals. Therefore, prior to this step, particle elemental composition has to be quantified.

When quantification of individual particle XEDS spectra is concerned, the use of conventional methods for bulk and thin polished materials (Castaing, 1951) imposes some critical limitations, and proper adjustments and assumptions for the theoretical treatment of X-ray generation and losses in the particulate matrix are needed (Armstrong and Buseck, 1975; Van Dyck et al., 1984; Choˇl et al., 2005 and 2007).

In addition to bulk matrix effects, the particle size and shape play a major role in the mass, absorption and fluorescence effects of particulate matrices (Fletcher et al., 2011).

In this study, the mass effect (induced by particle thickness lower than the spot size of primary electron beam) was considered negligible. Dust particles selected for quantification, indeed, show an equivalent projected area diameter (assumed as particle thickness according to Kandler et al., (2007)) above 2µm, that is far larger than the spot size used (0.3 ÷ 0.4 µm average). However, energy losses due to particle absorption and fluorescence effects cannot be neglected. Among methods described in literature to quantify environmental particles by XEDS microanalysis (Fletcher et al., 2011), the particle standard approach was adopted in this

work. In particular, an internal standard was used; by this choice, particle matrix effects are included in the quantification process, and the conventional standard-based quantification method still can be used (Castaing's first approximation corrected for bulk matrix effects by the ZAF algorithm). Full details of this approach are described in Appendix I of supplementary materials.~~Apportionment of individual dust particles analyzed by SEM XEDS can be carried out by matching XEDS spectra of particles to those of pure minerals. However, XEDS spectra of some minerals can be not available; in this case, apportionment can be performed by matching the quantified elemental composition of particles with that of pure minerals.~~

~~Therefore, prior to the apportionment procedure, particle elemental composition had to be quantified. When quantification of individual particle XEDS spectra is concerned, the use of conventional methods for bulk and thin polished materials (Castaing, 1951) imposes some critical limitations, and proper adjustments and assumptions for the theoretical treatment of X-ray generation and losses in the particulate matrix are needed (Armstrong and Buseck, 1975; Van Dyck et al., 1984; Choël et al., 2005 and 2007).~~

~~In addition to bulk matrix effects, the particle size and shape play a major role in the mass, absorption and fluorescence effects of particulate matrices (Fletcher et al., 2011). In this study, the mass effect (induced by particle thickness lower than the spot size of primary electron beam) was considered negligible. Dust particles selected for quantification, indeed, show an equivalent projected area diameter (assumed as particle thickness according to Kandler et al., (2007)) above 2µm, that is far larger than the spot size used (0.3 ÷ 0.4 µm average). However, energy losses due to particle absorption and fluorescence effects cannot be neglected. Among methods described in literature to quantify environmental particles by XEDS microanalysis (Fletcher et al., 2011), the particle standard approach was adopted in this work. In particular, an internal standard was used; by this choice, particle matrix effects are included in the quantification process, and the conventional standard based quantification method still can be used (Castaing's first approximation corrected for bulk matrix effects by the ZAF algorithm).~~

~~First, high-counts spectra of particles analyzed manually in the dust sample matrix (as described in Sect. 2.2) were quantified by the standard based routine available from EDAX control v. 3.3 package (Newbury and Ritchie, 2013); to this aim, the pure minerals available from EDAX Library have been used as standards. Long acquisition time and high counts of~~

these spectra are expected to minimize the statistical error of quantification (Goldstein et al., 1986). From the EDAX quantification routine, the element Z (atomic number), A (absorption) and F (fluorescence) correction factors, related to the influence of the particulate matrix on X-ray losses of individual particles, are obtained for each analyzed particle of a sample.

Element ZAF mean values, differentiated by dust sample, were then obtained by averaging, within each sample, ZAF values of all analyzed particles. Finally, the sample-specific mean ZAF values were used in the quantification of particle spectra obtained by automated microanalysis. The conventional standard-based ZAF-corrected Castaingôs method was used also in this case; however, the standard element concentration and ZAF were those of the manually-analyzed particles. By this procedure, indeed, manually analyzed particles could be assumed as internal particle standard, on a sample-specific base. The reliability of quantification of manually analyzed particles, by Castaingôs first approximation approach, was evaluated in terms of accuracy with respect to mineral standards available from the EDAX Library. Details and results are discussed in Sect. 3.1.1.

Particles showing total sum of element percent weight (%wt) below 50 (including oxygen estimated by element oxides) were not further considered in the rest of the study.

Reference XEDS spectra and elemental composition of pure minerals, to be used for particle apportionment, were obtained either from the EDAX Library (biotite, clorite, calcite, diopside, kaersutite, olivine, plagioclase and quartz) or by the RRUFF project (Downs, 2006) and GEOROC (Sarbas and Nohl, 2008) open-source databases, available on the web. Minerals collected from Central Italy were preferred where possible.

Spectral matching was performed by the chi square test for spectral goodness of fit included in the Library matching v.3.3 application (EDAX Inc., 2000). In cases where spectral matching couldnôt be performed, apportionment of particles to mineral species was obtained on the basis of the best fit of the dust particle %wt element composition versus the composition of pure minerals, by single linear regression analysis (SLR). The reliability of the internal standard approach has been evaluated by assessing the consistency of the apportionment to mineral species (which directly depends on results of quantification by internal standard approach) with XRD analysis.

Apportioned mineral particles of the volcanic and travertine dusts were then used to investigate the microphysical, optical and radiative properties of the PM10 lithogenic dust of Rome.

2.4 Size distribution

In this work, the assumption of particle sphericity has been adopted, due to the requirements of the 6SV code for radiative transfer modelling. Therefore, ~~P~~physical size of particles was assumed as the diameter of the equivalent spherical cross sectional area (ESD) (Reid et al., 2003; Kandler et al., 2007; Choy l et al., 2007) measured by SEM. Then, mineral density was assigned to apportioned particles; volume, mass and aerodynamic diameter were consequently calculated (Kulkarni et al., 2011). On this basis, the volume size distributions of most representative mineral species observed in this study (kaolinite, quartz, feldspar and calcite) have been built.

Formattato: Tipo di carattere: Tedesco (Germania)

2.4.1 Probability density function

The probability density functions (PDF) of the volcanics and travertine PM_{10} dust were estimated by fitting the frequency distribution of particle size to log-normal curve. Frequency distributions of volcanics and travertine were built on the basis of the 15 size bins of the GRIMM 1.108 optical particle counter (OPC). The fitting procedure was developed using the R-Project programming environment (R Core Team, 2013) and the routine was implemented by a nonlinear regression model based on a weighted-least-squares function (Ritz & Streibig, 2008)~~the routine was implemented by a general-purpose optimization based on Nelderï Mead algorithm (Nash, 1990)~~.

The procedure attended to minimise the deviation between observed distribution and log-normal model. This is expressed by the equation (Davies, 1974):

$$\frac{dN(r)}{d\log r} = \frac{N}{\sqrt{2\pi}\log\sigma}\exp\left(\frac{-1}{2}\left(\frac{\log r - \log r_m}{\log\sigma}\right)^2\right)$$

where N is the number of particles, r_m is the mean radius of particles, and $\hat{u}$ is the standard deviation of r. The uncertainty of each bin was estimated associating a Poisson error to the bin weight (Liley, 1992), that is calculating the square root of the total counts of particles observed in each size range. Quality assurance of the fitted models was evaluated considering the ñchi squaredò index (G^2) in order to estimate the level of acceptance (Wilks, 2006).

This index is proportional to the sum of squares of the difference between each data point and the corresponding computed value. The level of acceptance was defined using the ɢ2 distribution tables.

2.5 Radiative transfer modelling

An atmospheric radiative transfer code was employed~~, generally used in the remote sensing~~, to retrieve the optical and radiative dust properties. The 6SV (Second Simulation of a Satellite Signal in the Solar Spectrum ï Vector) (Vermote et al., 2006; Kotchenova et al., 2008) is the new-generation open-source atmospheric radiative transfer model 6S (Second Simulation of a Satellite Signal in the Solar Spectrum), (Vermote et al., 1997). This code is able to retrieve optical properties of the aerosol and to model the atmospheric radiative field by using the aerosol microphysical properties, under the hypothesis of spherical and dry particles. Microphysical properties of aerosol required for the modeling are the size distribution and refractive index. Size distributions targeted to the type of aerosol can be introduced as input in the 6SV code. To this aim, frequency distributions of particle size of the volcanics and travertine PM_{10} were processed for curve-fitting, as described in Sect. 2.4.1. Log-normal curve parameters r and ů of the two dust types were thus used as inputs in the 6SV code.

The real and imaginary parts of the refractive index (r.i.) were assumed from literature. This choice was driven by the fact that the 6SV code requires as input the spectral trend of the real and imaginary parts of r.i., and these measurements were not available from our laboratory. Therefore, ~~T~~the refractive index of the ówater-insolubleô aerosol component reported in Kokhanovsky (2008) was associated to the volcanics dust of Rome area. This component is indeed defined as mainly dust, rich in water-insoluble minerals e.g. silicates, and is reported in literature in the spectral domain considered by the 6SV code. In the case of travertine dust, the calcite refractive index data reported by Ghosh (1999), Sokolik and Toon (1999) and Di Biagio et al. (2014) were used.

The 6SV code retrieves aerosol optical properties by the Mie Theory and simulates, afterword, the radiative modeling by solving the radiative transfer equation (RTE) in the solar spectral domain. By this way, the propagation of solar radiation in the Atmosphere/Earth coupled system can be completely described.

Runs of 6SV code were performed on a setting of parameters related to the site-specific meteorological and atmospheric conditions, and to the aerosol loading and microphysical properties. Concerning meteorological parameters, the profiles of temperature, pressure and humidity were assumed by the *1976 U.S. Standard* Atmosphere included in the 6SV code.

Atmospheric conditions were established in order to model the radiative field under daily *maximum Sun* elevation in Rome Area; a spring day, 12 May, at midday was thus selected. Columnar contents of water vapor and of ozone were fixed to 1.32 cm and 0.283 Db, respectively. To describe the aerosol loading, the aerosol optical thickness at 550 nm, τ_{550} (Vermote at al., 1997; Kaufmann et al., 1997; Bassani et al., 2010 and 2012) is commonly considered. The atmospheric profile of the aerosol is assumed to be exponential with a scale height of 2 km (Vermote at al., 1997). In this study, however, an higher value of aerosol optical thickness, $\tau_{550} = 0.7$, was chosen, in order to allow describing a scenario where the local geological dust loading has a major role when the radiative field in the atmosphere/earth coupled system is simulated.

Among optical properties, the single-scattering albedo and the asymmetry parameter were chosen, as they are crucial to perform analysis of the aerosol contribution on the radiative field (Dubovik et al., 2002; Kassianov et al., 2007).

Concerning the simulation of the radiative quantities, the downward irradiance was modelled, to the aim of performing a preliminary investigation on the radiative impact of the different dust types in the Earth-atmosphere coupled system. The volcanics and travertine PM_{10} local dust are expected to show significantly distinct microphysical properties, due to their compositional differences. Radiative modelling has been performed thus on the assumption of an atmosphere where the only aerosol component is volcanics or travertine dust, separately.

In order to evaluate the direct radiative effect at the surface of the two local dust components, the radiative forcing efficiency (RFE) at BOA has been considered. In a recent modelling study, Gomez-Amo et al. (2011) derives the RFE by using a radiative transfer code. In this study, the RFE has been computed for each component by the difference between the BOA flux simulated by 6SV code in case of atmosphere with and without the dust component in the 250 - 4000 nm spectral domain and normalized with respect to the AOT at 550 nm (Garcia et al., 2008). The comparison between the RFE of volcanic and travertine allows to analyse the

dependence of surface forcing from aerosol types (microphysical properties) and SSA independently from the aerosol loading (di Sarra, 2008, 2013; Di Biagio et al., 2010).

Results are showed in Sect. 3.5.2 and 3.5.3.

3 Results and discussion

Results of individual-particle XEDS spectra quantification and classification into mineral species are reported in Sect. 3.1 ï 3.3. In particular, the discussion concerns the reliability of microanalysis and of high-counts spectra quantification (Sect. 3.1), a principal component analysis (PCA) of particles elemental composition (Sect. 3.2), the ~~apportionment~~allocation into mineral classes and the reliability of quantification by the internal standard approach used in this work (Sect. 3.3). In Sect. 3.4 volume size distributions are discussed, and differences between calcite from a lithogenic source (travertine dust) and from an anthropogenic material (paved road dust) are also evidenced. Finally, in Sect. 3.5 the microphysical and optical properties, and the downward component of radiative flux at BOA (Bottom Of Atmosphere) in a volcanics ï rich or travertine ï rich atmosphere are discussed, with respect to the features of Rome area.

3.1 Reliability of XEDS microanalysis and quantification

In Table 1 (upper part) the repeatability of XEDS microanalysis and consistency with the ED-XRF analysis are reported. Repeatability was evaluated by triple field acquisitions (number of fields: 20 ÷ 30) from each PM_{10} dust sample. Large fluctuations around mean (% relative standard deviation) are observed for light (Na and Mg principally) and trace (Mn and Ti) elements. Consistency with previously obtained elemental profiles of the PM_{10} fraction (Pietrodangelo et al., 2013) by ED-XRF, was assessed by matching to the latter the percent weight element composition of micro-areas of the dust samples obtained by XEDS field microanalysis. Results indicate that the microanalysis is less reliable for Na, Mn and for Si and Mg in the siliciclastics sample, while in all other cases it shows a good agreement with ED-XRF bulk analysis.

Quantification results of manually acquired XEDS individual particle spectra are also reported in Table 1 (lower part), for kaersutite, quartz and calcite. Quartz and calcite represent

the compositional end-members of mineral species observed in the dust samples of this work. Kaersutite particles were frequently observed during manual acquisitions. As this silicate mineral include in its composition non-negligible presence (above 4 %wt) of the principal crustal elements (Al, Na, Mg, K, Ca and Fe), it has been assumed as reference term for the microanalysis of silicate particles. XEDS spectra of kaersutite, calcite and quartz particles are showed in Fig. 3S, 4S and 5S, respectively.

The element composition is reported in terms of element mass in the electron interaction volume at 20 KeV; the latter was estimated for quartz, kaersutite and calcite according to Potts (1987). Uncertainties of quantification are large for K, Na, Mn and Ti, as expected due to the poor sensitivity of XEDS microanalysis to light and/or trace elements, whereas they range 1 ÷ 10 % relative error for other elements. Element uncertainties reported in Table 1 were estimated following the approach by Ziebold (1967), after assigning the proper peak-to-background ratio to each element in each mineral particle. The compositional differences of individual particles of quartz, calcite and kaersutite, with respect to related bulk mineral standards, are also reported in Table 1 (last rows) in terms of absolute percent differences between the element % wt in the standard mineral and that in the mineral particle.

As expected from the uncertainties, major compositional differences with respect to mineral standards are observed in Na, Mn and Ti quantification of kaersutite; also the quantification of Ca differs largely from the mineral standard, both in kaersutite and in calcite particles.

3.2 Elemental composition of individual dust particles

Particles included in the data set are individually codified with respect to the respective dust source, so that they are traceable in the statistical processing of data. Comparing information extracted from a multivariate statistical analysis of this data set, on the dust type to which each particle is ascribed, to same information certainly known from particle coding in the same data set, allows the evaluation of soundness of the elemental composition data and, consequently, of the quantification approach applied to particle XEDS spectra.

To this goal, a principal component analysis (PCA) of the elemental ratios commonly used to discriminate among different mineral classes (Al/Ca, Fe/Ca, K/Ca, Mg/Ca, Ti/Ca, Si/Al, Si/Fe, Ti/Fe and Ti/Mn) was performed. The XLSTAT 7.5 statistical package (Addinsoft) was used, with Varimax rotation and extraction of the latent factors; results are showed in Fig. 1

and 2. Three latent factors with eigenvalue higher than unity explain 76% of the total variance of particle composition. The element/Ca ratios mainly contribute to the first factor (F1, eigenvalue 4.5), the Si/Al and Si/Fe ratios contribute to the second factor (F2, eigenvalue 1.8), while the Ti ratios are represented by the third factor (F3, eigenvalue 1.3). In Fig. 1, particle scores are reported in the F2 vs F1 and in the F3 vs F2 plots.

Particles described by the F1 are ascribed to volcanics and, in minor fraction, to siliciclastics dust. The latter are indeed described mainly by the F2. Finally, road dust and travertine particles are grouped by the F3. Marlstone particles were not included in the PCA and in the subsequent parts of the study, due to the smaller number of available data with respect to the other samples. To assess the soundness of the PCA solution, the relative Si and Ca abundance and the equivalent spherical volume (ESV) have been examined, within clusters identified by the F1, F2 and F3. In Fig. 2, the Si and Ca abundances of particles with factor score higher than unity on each of the three latent factors have been plotted with respect to the ESV.

Since the average mass fractions of Si and Ca, in SiO_2 and $CaCO_3$ respectively, are 0.47 and 0.4, the threshold of 0.4 can be used to discriminate qualitatively either between silica and silicates (for which Si abundance is expected roughly below 0.4), and similarly between calcite and other Ca-bearing particles. Median Si abundance of both volcanics and siliciclastics particles in F1 is 0.37÷0.39 (Fig. 2a); also Ca abundance is similar in both particle groups (below 0.1). Median values of particle ESV are 3 μm^3 (volcanics) and 3.5 μm^3 (siliciclastic), although a very large variability was measured. Upon the above considerations on the Si mass fraction in SiO_2, a silicate nature of these particles might be supposed. Particles grouped by the F2 (Fig. 2b) are mainly siliciclastic and only a minor fraction is ascribed to volcanics. All these particles share both the Si and Ca abundances (0.6 and 0.1, respectively), and the median ESV (3÷3.5 μm3), the latter being comparable with the ESV of F1 particles. Si abundances far above 0.4 suggest that these are silica particles. It should be also noted that, as particles in F1 and F2 show similar ESV but different Si abundance, differences in the particle density can be supposed between these two groups. Finally, particles with the highest score in F3 (Fig. 2c) are mainly ascribed to road dust and travertine samples and show Ca abundances around 0.4, which can be related to $CaCO_3$.

The PCA solution found on the XEDS data set of particle elemental composition is thus coherent with the real mineralogical nature (silicate or calcite) of particles, indicating that the

sample-targeted internal standard approach applied to the quantification of particle composition provided reliable results.

3.3 Mineralogy of samples and ~~apportionment~~allocation of individual particles

The mineralogical composition quantified by XRD analysis is reported in Table 2.

Main differences concern the increasing amount of calcite (volcanics < siliciclastic rocks < marlstones < travertine), the absence of inosilicates in siliciclastic rocks and travertine, the negligible amount of phyllosilicates in travertine and the considerable presence of quartz in siliciclastic rocks. All of these features are consistent with the geological processes involved in the formation of each rock type. Calcite is a geochemical marker of the sedimentary environment where rocks are formed and it is associated to the chemical precipitation of calcium carbonate. As a consequence of that, while its presence in volcanic rocks is negligible, in the marine deposits (marlstones) it is dominant and in the siliciclastic series it represents the second most abundant mineral component after phyllosilicates.

Moreover, it is the almost exclusive component of travertine, generated by the precipitation of CaCO3 near the hot hydrothermal springs of the Tivoli basin (Pentecost, 2005; Faccenna et al., 2010). ~~The silicate component of marlstones and siliciclastics dust suggests that weathering processes are mainly responsible of the PM_{10} fraction of these dust types. This is evident by the presence of both stable silicates (plagioclase and quartz), which in the sedimentary domains can be ascribed to debris phases, and phyllosilicates. The latter are dominant also in the mineralogical composition of the volcanics dust, indicating once more the importance of chemical weathering. As an example, in the volcanics PM_{10} the kaolinite has been frequently observed, evidencing the possible occurrence of the hydrolysis reaction of feldspars (Jackson et al., 2010).~~ The mineralogical composition of the silicate component in marlstones and siliciclastics dust is strictly related to the originating materials. Rock-forming processes (erosion, fluvial and marine transport, sedimentation) support, in this case, the presence in the PM_{10} fraction, as detected by XRD, of stable silicates (plagioclase and quartz), the reduced presence of inosilicates and the presence of alteration by-products, such as phyllosilicates. Different processes must be considered in volcanic rocks, which explain the mineralogical composition of silicates observed in the PM_{10} resuspended from this geological material; specifically, crystallization is the main responsible process, in this case. Thus, the

presence of most minerals observed in the PM_{10} from volcanic rocks is coherent with the magmatological framework of Central Italy. Differently from the above considerations, however, the association kaolinite ï quartz, observed by SEM XEDS microanalysis in this PM_{10} dust type, has to be ascribed to rock alteration (weathering). In this case quartz is thus the product (with kaolinite) of the hydrolysis reaction of feldspars (Jackson et al., 2010), and not a crystallization-derived phase.

~~This process is well described by the association kaolinite ï quartz, observed by SEM XEDS microanalysis. In this case thus the quartz is not a crystallization-derived phase, but a weathering by-product.~~

Considering the results of the ~~apportionment~~allocation procedure (Sect. 2.3), mineral particles in the PM_{10} dust samples were mainly classified as: phyllosilicates (kaolinite, smectite and micas), representing more than half of the silicate (non-quartz) fraction of the totality of samples, tectosilicates (feldspar, chabazite, leucite and plagioclase) and inosilicates (clinopyroxene and amphibole), which contribute comparably to the rest of silicate fraction, quartz and calcite. About 65% (percent abundance) of total phyllosilicates are found in the volcanics, being mainly kaolinite (observed in the volcanics only) and 60% of total observed smectite. Micas are also frequently observed, mainly in the siliciclastics sample. Concerning tectosilicates, the overall contribution apportioned to the PM_{10} of each geological domain and of road dust has been found to be 47% in the volcanics, 20% in the siliciclastic rocks, 33% in the road dust, while it appears negligible in the marlstones. Inosilicates were observed in similar amounts, and solely in the volcanics and in the road dust. About half of quartz particles identified in the totality of PM_{10} dust samples is apportioned to siliciclastic rocks, while volcanics, marlstone and road dust provide equally to the remaining fraction. Finally, within the non-travertine sedimentary rocks of this study, the marlstones provide the most important contribution of calcite particles in the PM_{10} fraction (ab. 35%), while the contribution of siliciclastic rocks is around 8%. Similar contributions than marlstones are also apportioned to road dust. These results, obtained by the ~~apportionment~~allocation procedure, are in good agreement with the mineralogical composition by XRD (Table 2).

To assess the reliability of ~~apportionment~~allocation, a mass closure approach was used.

The particulate mass fraction of each mineral group in the PM_{10} (sum of particles mass within a mineral group, per dust sample) was estimated from results of the ~~apportionment~~allocation after SEM XEDS microanalysis. Afterwards, the PM_{10} weight percent composition of the

total silicate (including quartz) content and of the calcite content were calculated; these quantities were then compared to the corresponding quantity obtained by XRD analysis of the 50μm sieved fraction of each dust sample, as reported in Fig. 3.

Although the travertine was not analyzed by XRD, since it can be considered a pure calcite term (Pentecost, 2005), results of the ~~mass apportionment by~~ SEM XEDS microanalysis of the travertine dust have been reported for this sample too. In all dust samples (excluding the case of travertine), a good comparability with analytical results of mineral composition by XRD are observed for mass estimates obtained from the ~~apportionment~~allocation of individual particles. Besides indicating that the ~~apportionment~~allocation procedure produced reliable results, this also suggests that the silicate and calcite contents of the PM_{10} and of the 50μm sieved fractions of dust are likely similar, as yet reported in literature (Rashki et al., 2013).

3.4 Connections between geochemical processes of rock sources and the PM_{10} fraction of minerals

The size distribution of re-suspended geological materials is influenced by two important contributions: the physical properties of particles (e.g. size and density), which affect the dust ~~re-suspension~~resuspension and transport; and the geological features of the rock source, which determine the particle mineralogical identity. In this view, size distribution of the PM10 fraction has been discussed either for individual mineral species (quartz, kaolinite, feldspars and calcite), or for the overall local lithogenic dusts (volcanics, siliciclastic rocks and travertine); in the latter case the totality of mineral particles identified in each dust type was considered. In Sect. 3.4.1, size distributions of individual mineral species have been investigated with respect to the clay fraction according to Claquin et al. (1999), Nickovic et al. (2012), and Journet et al. (2014), while in Sect. 3.4.2 volume distributions (Formenti et al., 2014) of mineral species and of lithogenic dusts are discussed.

3.4.1 Clay fraction of minerals

In this part of the study the classified mineral particles were treated with respect to the geochemical processes which they can be related to, with the aim of relating the size

distribution of each mineral species to the geochemical processes acting on the rocks to generate the PM_{10} fraction of that mineral species. Therefore particles are here named as: - phyllosilicates, including clay-minerals (kaolinite, illite, smectite and chlorite groups), and representing thus the contribution of weathering and pedogenesis to the ~~re-suspension~~resuspension from outcropping rocks; - óother silicatesô, including phases such as plagioclase, K-feldspar, pyroxene and quartz, which can be considered as crystallization products in volcanics rocks, or debris phases in sedimentary rocks; -calcite, differentiated by lithogenic and road dust particles. The approach of Claquin et al. (1999) was adopted in choosing mineral species for which the mass percentage in the clay fraction (particle size < 2 µm) was calculated, on the basis of the particle ESD. Mass percentages of mineral in the clay fraction of PM_{10} dust samples of this study were compared with those obtained by Journet et al. (2014) for the modelled global yearly average composition of airborne minerals. With respect to the latter (abbr. *gyac*), the mineral composition of the Rome local geological PM_{10} shows the following similarities, or discrepancies: 1. the amount of quartz in the clay fraction of the siliciclastic PM_{10} (20%) and of the volcanics PM_{10} (8%) is significantly higher compared to the *gyac* (4.9%); 2. feldspars in the clay fraction of both the volcanics (4%) and siliciclastic PM_{10} (2.5%) are comparable to feldspars in the *gyac* (3.6%); 3. kaolinite dominates the clay fraction of the volcanics PM_{10} (63%) and it is negligible in the other PM_{10} dust types (ca. 2.5%), while in the *gyac* it represents 24.1% of total mass; 4. smectite in the Rome local geological PM_{10} ranges 3 to 10%, that is lower compared to *gyac* (15.3%).

With respect to the mineralogical profiles of PM_{10} dust from sources located in North Africa (N.A.) and Saudi Arabia (S.A.) (Ganor et al., 2009), the dust samples of this study show the following differences: 1) large variability in terms of calcite content (up to 90% in travertine), compared to PM_{10} from N.A. and S.A. (20-30%); 2) large variability in terms of tectosilicates (up to 20% in volcanics) and clay minerals (up to 57% in volcanics) compared to PM_{10} from N.A. and S.A. (1-3% 30-40% respectively); amount of quartz comparable to that in PM_{10} from N.A. and S.A. (2-4%) in the case oft he siliciclastic PM_{10}, but significatively different in travertine (undetectable) and in volcanics (10%). Moreover, the presence of inosilicates is not reported for the PM_{10} from N.A. and S.A., while the latter show the presence of gypsum, not observed in the PM_{10} dust samples of this study.

Considering the distribution of particles in the clay and non-clay (ESD > 2 µm) fractions of the mineral PM_{10} of Rome area, main differences are observed between the volcanics and the

travertine types. In the volcanics PM_{10} the weathering by-products (quartz, kaolinite and smectite) are comparably distributed in the two size fractions, indicating that weathering processes produce either small grain-sized crystals, and altered phases which grow on the surface of large crystals, resulting in larger particles. The crystallization phases produced in the volcanics PM_{10} (feldspars and pyroxene) are instead enriched in the non-clay size, as implied in the crystallization process.

Source-related differences between natural calcite from travertine and calcite from road dust were also evidenced. The clay/non-clay distributions of calcite in the PM_{10} of either the travertine dust and the road dust travertine-related, differ significantly from the clay/non-clay calcite distribution in the PM_{10} of road dust volcanics-related. While in the first case the calcite is comparably distributed in the clay/non-clay size, the mass percentage of this mineral in the road dust volcanics-related is higher in the clay size (80%) than in the coarser size (60%). Since the presence of calcite in the volcanics PM_{10} is negligible, calcite content in the PM_{10} road dust collected in the volcanics can only be ascribed to the asphalt contribution.

It is thus reasonable that this anthropogenic source enrichs the size fraction below 2 µm (ESD) of calcite, more than the coarser one. This effect is less evident, instead, in the road dust travertine-related, where the lithological influence of travertine rocks assumes a major role in the clay/non-clay distribution of calcite.

3.4.2 Volume size distribution of the PM_{10} fraction: minerals and lithogenic dust types

The volume size distributions of quartz, feldspars, kaolinite and calcite are reported in Fig. 4 versus the aerodynamic diameter (a.d.); in this figure, particles have been grouped with respect to belonging to a given mineral species, without differentiating by geological domain. Fig. 4a shows the distributions of kaolinite, quartz and feldspars, while in Fig. 4b distributions of calcite in the two different road dust types and in travertine are shown.

Volume distributions of the considered silicates are unimodal, with overlapping maxima around 5 µm. Main differences are in the peak width: weathering minerals, such as kaolinite, show a broader curve, compared to minerals from crystallization phases, e.g. feldspars. This is coherent with the above described action of the weathering, of generating particles either in the clay-fraction, and in the coarser size, which contributes to broaden the size range.

Quartz shows an intermediate behaviour, due to different processes acting on quartz formation: weathering in the volcanics, crystallization in the siliciclastics.

The different nature of geochemical processes affects also volume distributions of the overall lithogenic dust types (Fig. 4c). Particularly, volcanics and siliciclastics dusts show broader distribution than travertine, due to the dominance of weathering, in the formation of lithogenic PM_{10} from volcanic and siliciclastic rocks, with respect to the importance of crystallization in the travertine domain.

More defined differences are highlighted among the volume distributions of calcite from lithogenic or anthropic source: in PM_{10} from travertine, the volume distribution of calcite shows a very narrowed shape, with maximum at 5 µm. Conversely, calcite of both road dust types shows broader distributions, extended to finer sizes, especially in the case of the volcanics-related road dust. In the latter, the curve is bi-modal with maxima at 3.8 µm and 1.8 µm, while in the travertine-related it is unimodal, with maximum at 5.3µm similarly to calcite in travertine. The lithogenic or anthropic nature of processes tuning calcite size also influence the height of volume distributions of calcite.

In the first case, calcite particles mainly originate from crystals formed in the precipitation of calcium carbonate, as explained in Sect. 3.3; the variability of particle size is thus limited by chemical ï physical conditions which rule travertine formation. In the second case, the variety of mechanical solicitations affecting the surface of paved roads, e.g. abrasion by vehicle riding, is described by a wider particle size range.

Discrepancies observed within volume distribution curves of Fig. 4 suggest also that individual particle densities may differ within the same silicate species or within calcite from different dust sources. It is acknowledged that the density of mineral particles may range significantly due to the petrological conditions (chemistry, kinetics and thermodynamics involved in the crystallization process) associated to the different crystallization phases, by which mineral particles are formed.

In addition, some general considerations can be given on the particle density, by taking into account the distribution of particle mass percentage (discussed in Sect. 3.4.1) and ESD, with respect to the below/above 2 µm size threshold (coherently with the clay / non-clay distribution). Decreasing particle density should be expected from first to last of the following cases: 1. both mass percentage and ESD of particles mainly distributed below 2 µm; 2. mass percentage mainly observed below the 2 µm size and ESD comparably distributed with

respect to this threshold; 3. both mass percentage and ESD mainly distributed in the size fraction above 2 µm. In Fig. 4, first case can be related to the calcite of road dust volcanics-related (80% of particles showing ESD < 2 µm), while second case applies to quartz and kaolinite, and last case to feldspars and travertine calcite (60% and 80%, respectively, of particles showing ESD > 2 µm).

Height differences among volume distributions of the dust types can be thus explained in connection with the different presence of a given mineral species in a dust type. In particular, while the content of kaolinite is higher in the volcanics than in siliciclastic dust, feldspars and quartz are more abundant in the latter. It is thus possible that these minerals play contrasting roles in defining the average particle density of siliciclastic dust, and consequently its volume distribution.

3.5 Microphysical, optical and radiative properties of the volcanics and travertine PM_{10} dust in the Rome area

3.5.1 Microphysical properties

In Fig. 5 results ~~are showed~~ of the fitting procedure to log-normal curve, applied to volcanics and travertine size distribution, are shown. ~~to obtain dust-specific log-normal curves.~~ The curves are reported with respect to the particle physical radius, as required by the 6SV radiative transfer code. The computed ñchi squaredò (χ^2) of fitting are respectively 0.34 for volcanics and ~~0.59~~ 0.69 for travertine. Considering twelve degrees of freedom corresponding to the 13 size bins of the optical particle counter, both fitting are below the level of significance of 99.5%. It is thus possible to refuse the null hypothesis that these curves cannot be fitted to a log-normal function. The following r_m and σ values of the volcanics and travertine size distributions are used thus, as input parameters of the Log-normal function (Eq. 1):

$r_m^{volc} = 1.64 \pm 0.29$ µm, $\sigma^{volc} = 1.85 \pm 0.23$ µm;

$r_m^{trav} = 1.39 \pm 0.72$ µm, $\sigma^{trav} = 2.34 \pm 0.46$ µm.

Results of fitting are in line with findings discussed by Mahowald et al. (2014).

The other microphysical property required for 6SV run is the refractive index. In Fig. 6 the real (n) and imaginary (k) part of the refractive index have been interpolated at the 6SV twenty wavelengths (350; 400; 412; 443; 470; 488; 515; 550; 590; 633; 670; 694; 760; 860; 1240; 1536; 1650; 1950; 2250; 3750 nm), following the spectral data of water-insoluble (Kokhanovsky, 2008; WCP-112, 1986) and calcite-rich dust (Ghosh, 1999) refractive index, respectively related to volcanics and travertine. While the spectral trend of volcanics refractive index follows the commonly adopted trend used in the radiative transfer modelling (RTM) of the dust component (Kokhanovsky, 2008), the travertine dust, being mainly composed of calcite, is a non-absorbing aerosol in the spectral range considered in this study, as in this range the imaginary part of calcite refractive index is close to zero (Sokolik and Toon, 1999; Ghosh, 1999; Di Biagio et al., 2014 ~~é ,Ghosh, 1999~~).

3.5.2 Optical properties

Optical properties of the volcanics and travertine contribution to Rome local mineral dust have been modeled in the twenty wavelengths of the 6SV code. In Fig. 7 the single-scattering albedo (SSA) and the asymmetry parameter (g) are shown, which are critical to analyze the aerosol-induced at-ground radiative flux (Kassianov et al., 2007). The lower SSA of volcanics, with respect to travertine, attests that the volcanics dust absorbs the solar radiation in the VISible (VIS) spectral domain, as commonly expected for mineral dust. Conversely, the SSA of travertine indicates that this dust type is a non-absorbing particulate. In Fig. 7b the spectral dependence of the asymmetry parameter (g) is showed for the volcanics and the travertine. As g is higher in the volcanics, in this dust type particles show higher forward scattering than in the travertine, mainly in the Near-InfraRed (NIR) spectral domain. These findings suggest that the local geological dust of the Rome area affects both the VIS and NIR spectral domains; consequently an influence on the radiative field is expected as well.

3.5.3 Downward radiative flux at Bottom Of Atmosphere (BOA)

The radiative modeling has been focused on the downward component of the radiative impact at BOA due to the volcanics and travertine dust in Rome area. This part of the study represents a preliminary investigation of the direct radiative effect of the local dust component on the solar radiation at ground. In Fig. 8a the influence of both local dust types to the downward BOA solar irradiance (I) in the VIS and NIR spectral domain is shown. In order to

Formattato: Non aggiungere spazio tra paragrafi dello stesso stile

evaluate the spectral dependence of the irradiance on the mineralogical composition of dust, the volcanics/travertine ratio is reported in Fig. 8b. In the VIS domain, the irradiance seems not to be affected by the mineralogical composition, as the BOA downward irradiance trends of two dust types almost overlap. However, in the NIR a sharp discrimination between the radiative impact of the volcanics and that of the travertine dust is revealed. Finally, the BOA downward flux obtained by integrating the downward solar irradiance over the solar spectral domain (250 - 4000 nm) is reported in Fig. 9. Both volcanic and travertine dusts leave the direct component unchanged, while the diffuse component depends strongly on the mineral composition. The scattered radiation of an atmosphere rich in travertine dust shows an higher diffuse component than in the case when a volcanics ï rich atmosphere is considered. As a matter of fact, in the Rome site the total BOA downward flux is greater for an atmosphere where the only dust component is the travertine dust with respect to the sole presence of volcanic dust.

The evaluation of the radiative budget at surface of the local mineral dust in Rome area has been performed computing the RFE. The RFE is calculated by simulating the total BOA downward flux with the local dust component in three conditions of AOT at 550 nm (0.2; 0.5; 0.7), to estimate the uncertainty on the simulated RFE. The results highlight the stronger cooling effect at the surface in case of volcanic (-293 ± 17 W/m2) respect to travertine (-139 ± 7 W/m2) with uncertainties lower than 5%.

The aerosol radiative behaviour follow the general trend explained in Gomez-Amo et al., (2011), that is aerosols with high SSA (low absorption, travertine in case) produces a decrease in the absolute value of RFE, with respect to aerosols t characterized by high absorption, like the volcanics.

These results need to be confirmed by a more in-depth analysis on the influence of the local geological dust re-suspended from topsoil on the Earth ï atmosphere radiative balance, in Rome area. ~~Nevertheless, the charge of differences existing in the Rome local mineral dust composition on the variability of optical and radiative properties of the airborne aerosol appears as a key issue, to be further considered in the radiative balance analysis.~~

Formattato: Non aggiungere spazio tra paragrafi dello stesso stile

4 Conclusions

In this work, a knowledge gap was faced, which concerns how, and to which extent, the

mineral dust locally re-suspended from rocks outcropped in a site/area may influence the composition of airborne aerosol, the direct interaction (light scattering and absorption) of the aerosol with solar radiation, and the radiative flux at BOA (Bottom Of Atmosphere), within the same source area of dust. To this goal, a methodology was developed, which is suitable for general application; nevertheless, results reported here are intrinsically narrowed to the features of Rome area. Investigation was carried following three paths: site-specific analysis of the geochemical and mineralogical environment, individual-particle based instrumental analysis aimed at determining the mineralogical and microphysical properties of dust, and modelling of the dust radiative effects with respect to optical features.

Main results concern relationships found between: 1.geochemical processes acting on the source rocks and mineral species associated to particles in the re-suspended PM_{10} fraction of different local dust types; 2. mineral composition of the PM_{10} dust and variability of dust microphysical properties (refractive index and size distribution); 3. dust-specific optical properties (single-scattering albedo and asymmetry parameter) of the PM_{10} fraction, and total downward flux at BOA in the VISible and Near Infrared (NIR) spectral domains.

First issue was discussed on all major outcropped domains in the Rome area (volcanic rocks, siliciclastic rocks, limestones, marlstones and travertine), and on the distinction between calcite from lithogenic source and calcite from paved road dust, while second and third issues focused on the compositional end-member of local dust types (volcanics and travertine).

With the exception of pure calcite (associated to PM_{10} from the travertine domain (Tivoli basin), and from road dust), PM_{10} dust types of the studied area show silicate-prevalent or calcite-prevalent compositions, depending on the outcropped source rocks: volcanics or siliciclastics in the first case, marlstones or limestones in the second case.

Rock weathering processes tune the size and mineral identity of PM_{10} particles in the silicate-prevalent dust types, more than other processes (e.g. debris formation, crystallization). On the other side, chemical precipitation of $CaCO_3$ influences mainly the particle composition of calcite-prevalent dust types. These differences reflect in the volume distributions, either of individual mineral species (kaolinite, quartz, feldspars, calcite), or of dust types.

Weathering processes can be related to larger size variability observed for some mineral species (e.g. kaolinite and quartz), with respect to feldspars and to lithogenic calcite.

In the lithogenic PM_{10} of Rome area, these minerals are instead mainly associated to crystallization or to $CaCO_3$ precipitation, occurring under defined chemical, kinetic and thermodynamic conditions which limit particle size and result in narrow volume distribution.

Differences observed between calcite from lithogenic source and calcite from road dust suggest a major role of the variability of mechanical solicitations from vehicular riding on the particle size of road dust calcite. Volume distribution of the latter interestingly shows bimodal shape, broader width and larger contribution to fine fraction, differing significantly from lithogenic calcite and from other investigated mineral species.

These findings indicate that the microphysical properties of different crustal components (e.g. road dust, dust from building activities, transported mineral dust, etc.) may differ consistently with source type; optical properties are reasonably expected to differ consequently.

Spectral trends of the complex refractive index related to volcanics and travertine PM_{10}, in the VIS and NIR domains, show that travertine PM_{10} is a non-absorbing dust, opposite to volcanics PM_{10}. We showed that these differences influence the diffuse component of BOA downward flux, which is higher in the simulated case of a travertine-rich atmosphere, coherently with the non-absorbing behavior of this dust type.

Finally, it is important to underline that above results could be assessed only by considering the entire solar spectral domain, instead of limiting the investigation to the VIS region.

The radiative effects of the two components in the ~~2~~350 - 3750~~4000~~ nm spectral domain have been evaluated by the RFE; results show higher efficiency of volcanic (-293 ± 17 W/m2) in surface cooling effect, with respect to travertine (-139 ± 7 W/m2), as expected for aerosol with SSA smaller than 1 (Di Biagio et al., 2010), that is the volcanics dust in this case.

Further research on these issues is needed, thus, as it may aid improving knowledge on the local effects of the presence of different crustal (natural or anthropic) components of aerosol at a specific site/area, in terms of aerosol interaction with solar radiation and radiative effects at BOA.

Acknowledgements

Thanks are due to Sergio Lo Mastro (Roma Tre University, Department of Geology, Rome, Italy), for X-ray diffraction analysis of the dust samples of this study. The authors are also grateful to Andrea Valdrè (FEI Company, U.S.), for his valuable scientific and technical advice with SEM XEDS microanalysis. Finally, ~~-~~we are grateful to Alcide di Sarra (ENEA, Laboratory for Earth Observations and Analyses) for helpful comments and suggestions that greatly improved the radiative transfer issues in the manuscript.

References

Aimar, S., Mendez, J. M., Funk, M., Buschiazzo, D. E.: Soil properties related to potential particulate matter emissions (PM10) of sandy soils, Aeolian Res., 3, 437-443, 2012.

Armstrong, J. T. and Buseck, P. R.: Quantitative chemical analysis of individual microparticles using the electron microprobe: theoretical , Anal. Chem., 47, 13, 2178-2192, 1975.

Bassani, C., Cavalli, R., Antonelli, P.: Influence of aerosol and surface reflectance variability on hyperspectral observed radiance, Atmos. Meas. Tech., 5, 1139ï 1203, doi:10.5194/amt-5-1193-2012, 2012.

Bassani, C., Cavalli, R.M., Pignatti, S.: Aerosol optical retrieval and surface reflectance from airborne remote sensing data over land, Sensors, 10, 6421ï 6438, doi:10.3390/s100706421, 2010.

Bergstrom, R. W., Russell, P. B., and Hignett, P.: Wavelength Dependence of the Absorption of Black Carbon Particles: Predictions and Results from the TARFOX Experiment and Implications for the Aerosol Single Scattering Albedo, J. Atmos. Sci., 59, 567-577, 2002.

Bevington, P. R. and Robinson, D. K.: Data Reduction and Error Analysis for the Physical Sciences, 2d Ed., McGraw-Hill, New York, 1992.

Buseck, P. R. and Pósfai, M.: Airborne minerals and related aerosol particles: Effects on climate and the environment, Proc. Natl. Acad. Sci. USA, 96, 3372ï 3379, Colloquium Paper, 1999.

Caquineau, S., Gaudichet, A., Gomes, L., Legrand M.: Mineralogy of Saharan dust transported over northwestern tropical Atlantic Ocean in relation to source regions, J. Geophys. Res., 107, D15, 4251, doi: 10.1029/2000jd000247, 2002.

Castaing, R.: Application des sondes électroniques à une méthode d'analyse ponctuelle chimique et cristallographique: publication ONERA (Office national d'études et de recherches aéronautiques/ Institute for Aeronautical Research) N. 55 (PhD Thesis), University of Paris, Paris,1952.

Choobari, O. A., Zawar-Reza, P., Sturman, A.: The global distribution of mineral dust and its impacts on the climate system: A review, Atmos. Res., 138, 152ï 165, 2014.

Choýl, M., Deboudt, K., Flament, P.: Evaluation of quantitative procedures for x-ray microanalysis of environmental particles, Microsc. Res. Techniq., 70, 11, 996-1002, doi: 10.1002/jemt.20510, 2007.

Formattato: Inglese (Stati Uniti)

Choël, M., Deboudt, K., Osán, J., Flament, P., Van Grieken, R.: Quantitative Determination of Low-Z Elements in Single Atmospheric Particles on Boron Substrates by Automated Scanning Electron Microscopy-Energy-Dispersive X-ray Spectrometry, Anal. Chem., 77, 5686-5692, 2005.

Claquin, T., Schulz, M., Balkanski, Y. J.: Modeling the mineralogy of atmospheric dust sources, J. Geophys. Res., 104, D18, 22,243-22,256, 1999.

Cosentino, D., Cipollari, P., Di Bella, L., Esposito, A., Faranda, F., Giordano, G., Gliozzi, E., Mattei, M., Mazzini, I., Porreca, M., Funiciello, R.: Tectonics, sea level changes and palaeoenvironments in the early Pleistocene of Rome (Italy), Quaternary Res., 72, 143-155, 2009.

Costantini, E. A. C., Urbano, F., Aramini, G., Barbetti, R., Bellino, F., Bocci, M., Bonati, G., Fais, A., LôAbate, G., Loj, G., Magini, S., Napoli, R., Nino, P., Paolanti, M., Perciabosco M., and Tascone, F.: Rationale and methods for compiling an Atlas of desertification in Italy, Land Degrad. Develop., 20, 261ï 276, doi: 10.1002/ldr.908, 2009.

DôAlmeida, G. A., Koepke, P., and Shettle, E. P.: Atmospheric Aerosols, Global Climatology and Radiative Characteristics. A. Deepak Publishing, Hampton, VA, 1991.

DôAlmeida, G. A.: On the variability of desert aerosol radiative characteristics, J. Geophys. Res., 92, D3, 3017-3026, 1987.

Davies, C. N.: Size distribution of atmospheric particles, Aerosol Sci., 5, 293-300,1974.

Di Biagio, C., di Sarra, A., Meloni, D., Monteleone, F., Piacentino, S., Sferlazzo, D.: Measurements of Mediterranean aerosol radiative forcing and influence of the single scattering albedo, J. Geophys. Res., 114, D06211, doi:10.1029/2008JD011037, 2009.

Di Biagio, C., di Sarra, A., Meloni, D.: Large atmospheric shortwave radiative forcing by Mediterranean aerosol derived from simultaneous ground-based and spaceborne observations, and dependence on the aerosol type and single scattering albedo, J. Geophys. Res., 115, D10209, doi:10.1029/2009JD012697, 2010.

Di Biagio, C., Boucher, H., Caquineau, S., Chevaillier, S., Cuesta, J., and Formenti, P.: Variability of the infrared complex refractive index of African mineral dust: experimental estimation and implications for radiative transfer and satellite remote sensing, Atmos. Chem. Phys., 14, 11093ï 11116, doi: 10.5194/acp-14-11093-2014, 2014.

Formattato: Tipo di carattere: Non Grassetto

Formattato: Tipo di carattere: Non Grassetto

di Sarra, A., Pace, G., Meloni, D., De Silvestri, L., Piacentino, S., Monteleone, F.:Surface shortwave radiative forcing of different aerosol types in the central Mediterranean, Geophys. Res. Lett., 35, L02714, doi:10.1029/2007GL032395, ~~2008.~~

di Sarra, A., Fuà, D., Meloni, D.: Estimate of surface direct radiative forcing of desert dust from atmospheric modulation of the aerosol optical depth, Atmos. Chem. Phys., 13, 5647-5654, doi:10.5194/acp-13-5647-2013, 2013.

Dobrzhinsky, N., Krugly, E., Kliucininkas, L., Prasauskas, T., Kireitseu, M., Zerrath, A., Martuzevicius, D.: Characterization of desert road dust aerosol from provinces of Afghanistan and Iraq, Aerosol Air. Qual. Res., 12, 1209-1216, 2012.

Downs R. T: The RRUFF Project: an integrated study of the chemistry, crystallography, Raman and infrared spectroscopy of minerals, 19th General Meeting of the International Mineralogical Association in Kobe, Japan, July 23-28, O03-13, 2006.

Dubovik, O. and King, M. D.: A flexible inversion algorithm for retrieval of aerosol optical properties from Sun and sky radiance measurements, J. Geophys. Res.,105, D16, 20,673-20,696, 2000.

Dubovik, O., Holben, B., Eck, T. F., Smirnov, A., Kaufman, Y. J., King, M. D., Tanré, D., and Slutsker, I.: Variability of absorption and optical properties of key aerosol types observed in worldwide locations, J. Atmos. Sci., 59, 590-608, 2002.

Dürr, H. H., Meybeck, M., Dürr, S. H.: Lithologic composition of the Earthôs continental surfaces derived from a new digital map emphasizing riverine material transfer, Global Biogeochem. Cy., 19, GB4S10, doi:10.1029/2005GB002515, 2005.

Evans, R. D., Jefferson, I. F., Kumar, R., Hara-Dhand, K. O., Smalley, I. J.: The nature and early history of airborne dust from North Africa in particular the Lake Chad basin, J. Afr. Earth Sci., 39, 81ï 87, 2004.

Faccenna, C., Funiciello, R., Soligo, M.: Origin and deposition of the Lapis Tiburtinus travertine, in: The Colli Albani Volcano: Funiciello, R. and Giordano, G. Editors, Geological Society of London, 215, ISBN: 978-1-86239-307-3, 2010.

Falkovich, A. H., Ganor, E., Levin, Z., Formenti, P., Rudich, Y.: Chemical and mineralogical analysis of individual mineral dust particles, J. Geophys. Res., 106, D16, 18,029-18,036, 2001.

Feng, G., Sharratt, B., Wendling, L.: Fune particle emission potential from loam soils in a semiarid region, Soil Sci. Soc. Am. J., 75, 2262ï 2270, 2011.

Formattato: Tipo di carattere: Non Grassetto

Formattato: Tipo di carattere: Non Grassetto

Formattato: Non Evidenziato

Formattato: Tipo di carattere: (Predefinito) Times New Roman, 12 pt, Colore carattere: Nero, Inglese (Stati Uniti)

Formattato: Tipo di carattere: (Predefinito) Times New Roman, 12 pt, Colore carattere: Nero, Inglese (Stati Uniti)

Formattato: Tipo di carattere: (Predefinito) Times New Roman, 12 pt, Colore carattere: Nero, Inglese (Stati Uniti)

Fletcher, R. A., Ritchie, N. W. M., Anderson, I. M., Small, J. A.: Microscopy and microanalysis of individual collected particles, in: Aerosol Measurement: Principles, Techniques, and Applications, 3rd Ed.: Kulkarni, P., Baron, P.A. and Willeke, K. Editors, John Wiley & Sons Ltd, U.S., chapter 10, 195-198, 2011.

Formenti, P., Caquineau, S., Desboeufs, K., Klaver, A., Chevaillier, S., Journet, E., and Rajot, J. L.: Mapping the physico-chemical properties of mineral dust in western Africa: mineralogical composition, Atmos. Chem. Phys., 14, 10663ï 10686, doi:10.5194/acp-14-10663-2014, 2014.

Ganor, E., Stupp, A., and Alpert, P.: A method to determine the effect of mineral dust aerosols on air quality, Atmos. Environ., 43, 5463ï 5468, 2009.

Garcìa, O. E., Dìaz, A. M., Expòsito, F. J., Dìaz, J. P., Dubovik, O., Dubuisson, P., Roger, J.-C., Eck, T. F., Sinyuk, A., Derimian, Y., Dutton, E. G., Schafer, J. S., Holben, B. N., Garcìa, C. A.: Validation of AERONET estimates of atmospheric solar fluxes and aerosol radiative forcing by ground-based broadband measurements, J. Geophys. Res., 113, D21207, doi:10.1029/2008JD010211, 2008.

Geoportale Nazionale, http://www.pcn.minambiente.it/GN/ MATTMï Ministero dellôAmbiente e della Tutela del Territorio e del Mare, Italy, 2011.

Ghosh, G.: Dispersion-equation coefficients for the refractive index and birefringence of calcite and quartz crystals, Opt. Commun., 163, 1ï 3, 95-102, doi:10.1016/S0030-4018(99)00091-7, 1999.

Giampaolo, C. and Lo Mastro, S.: Analisi (semi) quantitativa delle argille mediante diffrazione a raggi X, In Fiore, S. (Editor.), Incontri Scientifici, Istituto di ricerca sulle argille, Vol. II, p 109-146 2000.

Gill, T. E., Zobeck, T. M., Stout, J. E.: Technologies for laboratory generation of dust from geological materials, J. Haz. Mat., 132, 1-13, 2006.

Goldstein, J. I., Williams, D. B., Cliff, G.: Quantitative x-ray analysis, in: Principles of Analytical Electron Microscopy: Joy, D. C., Romig Jr., A. D., and Goldstein, J. I. Editors, chapter 5, Springer U.S., ISBN: 978-1-4899-2039-3, 1986.

Gómez-Amo, J.L., Pinti, V., Di Iorio, T., di Sarra, A., Meloni, D., Becagli, S., Bellantone, V., Cacciani, M., Fuà, D., Perrone, M.R.: The June 2007 Saharan dust event in the central Mediterranean: Observations and radiative effects in marine, urban, and sub-urban environments, Atmospheric Environment, Volume 45, Issue 30,Pages 5385-5393, ISSN 1352-2310, doi:10.1016/j.atmosenv.2011.06.045, 2011.

Formattato: Tipo di carattere: Non Grassetto

Hansell Jr., R. A., Reid, J. S., Tsay, S. C., Roush T. L., and Kalashnikova, O. V.: A sensitivity study on the effects of particle chemistry, asphericity and size on the mass extinction efficiency of mineral dust in the earthôs atmosphere: from the near to thermal IR, Atmos. Chem. Phys., 11, 1527ï 1547, 2011.

~~Hsu, Y. and Divita, F.: SPECIATE 4.2, speciation database development documentation, final report, EPA/600-R-09/-38, 2009.~~

Jackson, M., Deocampo, D., Marra F., and Scheetz, B.: Mid-Pleistocene Pozzolanic volcanic ash in ancient Roman concretes, Geoarchaeology, 25, 1, 36-74, 2010.

Jeong, G. Y.: Bulk and single-particle mineralogy of Asian dust and a comparison with its source soils, J. Geophys. Res., 113, D02208, 4251-, doi: 10.1029/2007jd008606, 2008.

Journet, E., Balkanski, Y., and Harrison, S. P.: A new data set of soil mineralogy for dust-cycle modeling, Atmos. Chem. Phys., 14, 3801-3816, 2014.

Kalashnikova, O. V. and Sokolik, I. N.: Importance of shapes and compositions of wind-blown dust particles for remote sensing at solar wavelengths, Geophys. Res. Letters, 29, 10, 1398-, doi: 10.1029/2002GL014947, 2002.

Kalashnikova, O. V. and Sokolik, I. N.: Modeling the radiative properties of non-spherical soil-derived mineral aerosols, J. Quant. Spectrosc. Radiat. Transfer, 87, 137ï 166, 2004.

Kandler, K., Benker, N., Bundke, U., Cuevas, E., Ebert, M., Knippertz, P., Rodríguez, S., Schütz, L., Weinbruch, S: Chemical composition and complex refractive index of Saharan Mineral Dust at IzaŕÁa, Tenerife (Spain) derived by electron microscopy, Atmos. Environ., 41, 8058ï 8074, 2007.

Kandler, K., Schütz, L., Deutscher, C., Ebert, M., Hofmann, H., Jäckel, S., Jaenicke, R., Knippertz, P., Lieke, K., Massling, A., Petzold, A., Schladitz, A., Weinzierl, B., Wiedensohler, A., Zorn, S., Weinbruch, S.: Size distribution, mass concentration, chemical and mineralogical composition and derived optical parameters of the boundary layer aerosol at Tinfou, Morocco, during SAMUM 2006, Tellus, 61B, 32ï 50, 2009.

Karner, D. B., Marra, F., and Renne, P. R.: The history of the Monti Sabatini and Alban Hills volcanoes: groundwork for assessing volcanic-tectonic hazards for Rome, J. Volcanol. Geoth. Res., vol. 107, 185-219, 2001.

Kassianov, E. I., Flynn, C. J., Ackerman, T. P., and Barnard, J. C.: Aerosol single-scattering albedo and asymmetry parameter from MFRSR observations during the ARM Aerosol IOP 2003, Atmos. Chem. Phys., 7, 3341-3351, doi:10.5194/acp-7-3341-2007, 2007.

Kaufman, Y. J., Tanre, D., Gordon, H. R., et al.: Passive remote sensing of tropospheric aerosol and atmospheric correction for the aerosol effect, J. Geophys. Res., 102, 16,815ï 16,830, 1997.

Kim, H. K., Hwang, H. J., Un Ro, C.: Single-particle characterization of soil samples collected at various arid areas of China, using low-Z particle electron probe X-ray microanalysis, Spectrochim. Acta, Part B, 61, 393ï 399, 2006.

Kokhanovsky, A. A.: Aerosol Optics. Light Absorption and Scattering by Particles in the Atmosphere, Springer, Germany, ISBN 978-3-540-23734-1, 2008.

Kotchenova, S. Y., Vermote, E. F., Levy, R., and Lyapustin, A.: Radiative transfer codes for atmospheric correction and aerosol retrieval: Intercomparison study, Appl. Optics, 47, 2215ï 2226, doi:10.1364/AO.47.002215, 2008.

Krueger, B. J., Grassian, V. H., Cowin, J. P., Laskin, A.: Heterogeneous chemistry of individual mineral dust particles from different dust source regions: the importance of particle mineralogy, Atmos. Environ., 38, 6253ï 6261, 2004.

Kulkarni, P., Baron, P. A., and Willeke, K.: Fundamentals of single particle transport, in: Aerosol Measurement: Principles, Techniques, and Applications, 3rd Ed.: Kulkarni, P., Baron, P. A., and Willeke, K. Editors, John Wiley &Sons Ltd., U.S., chapter 8, 24-25, 2011.

Levin, Z., Ganor, E., Gladstein, V.: The effects of desert particles coated with sulfate on rain formation in the Eastern Mediterranean, J. Appl. Meteorol., 35, 1511-1523, 1996.

Liley, J. B.: Fitting Size Distributions to Optical Particle Counter Data, Aerosol Sci. Tech., 17, 2, 84-92, 1992.

Mahowald, N., Albani, S., Kok, J. F., Engelstaeder, S., Scanza, R., Ward, D. S., Flanner, M. G.: The size distribution of desert dust aerosols and its impact on the Earth system, Aeolian Res., 15, 53ï 71, 2014.

Meloni, D., Di Sarra, A., Pace, G., Monteleone, F.: Aerosol optical properties at Lampedusa (Central Mediterranean). 2. Determination of single scattering albedo at two wavelengths for different aerosol types, Atmos. Chem. Phys., 6, 715ï 727, 2006.

Moore, D. M. and Reynolds, R. C.: X-ray diffraction and the identification and analysis of clay minerals, Oxford University Press, Oxford, 1997.

Moreno, T., Amato, F., Querol, X., Alastuey, A., Elvira, J., Gibbons, W.: Bedrock controls on the mineralogy and chemistry of PM10 extracted from Australian desert sediments, Environ. Geol., 57, 411ï 420, doi:10.1007/s00254-008-1312-2, 2009.

Formattato: SpazioPrima: 0 pt, Aggiungi spazio tra paragrafi dello stesso stile, Interlinea singola, Regola lo spazio tra testo asiatico e in alfabeto latino, Regola lo spazio tra caratteri asiatici e numeri

Formattato: Tedesco (Germania)

Müller, T., Schladitz, A., Massling, A., Kaaden, N., Kandler, K., Wiedensohler, A.: Spectral absorption coefficients and imaginary parts of refractive indices of Saharan dust during SAMUM-1, Tellus, 61B, 79ï 95, 2009.

Nash, J. C.: Compact numerical methods for computers: linear algebra and function minimisation, 2nd Ed.. Adam Hilger, Bristol, 1990.

Newbury, D. E. and Ritchie, N. W. M.: Is Scanning Electron Microscopy/Energy Dispersive X-Ray Spectrometry (SEM/EDS) quantitative? Scanning, 35, 141ï 168, 2013.

Nickovic, S., Vukovic, A., Vujadinovic, M., Djurdjevic, V., Pejanovic, G.: Technical Note: High-resolution mineralogical database of dust-productive soils for atmospheric dust modeling, Atmos. Chem. Phys., 12, 845ï 855, 2012.

OAQPS Staff: Review of the National Ambient Air Quality Standards for Particulate Matter: Policy assessment of scientific and technical information, OAQPS Staff Paper, EPA-452/R-05-005, chapter 2, 2005.

Papayannis, A., Mamouri, R. E., Amiridis, V., Remoundaki, E., Tsaknakis, G., Kokkalis, P., Veselovskii, I., Kolgotin, A., Nenes, A., and Fountoukis, C.: Optical-microphysical properties of Saharan dust aerosols and composition relationship using a multi-wavelength Raman lidar, in situ sensors and modelling: a case study analysis, Atmos. Chem. Phys., 12, 4011ï 4032, 2012.

Peng, F. and Effler, S. W.: Suspended minerogenic particles in a reservoir: Light-scattering features from individual particle analysis, Limnol. Oceanogr., 52(1), 204ï 216, 2007.

Pentecost, A.: Travertine, Springer, U.S., chapter 7, 124, ISBN: 1-4020-3523-3, 2005.

Perrino, C., Canepari, S., Catrambone, M., Dalla Torre, S., Rantica, E., and Sargolini, T.: Influence of natural events on the concentration and composition of atmospheric particulate matter, Atmos. Environ., 43, 4766ï 4779, 2009.

Pietrodangelo, A., Salzano, R., Rantica, E., Perrino, C.: Characterisation of the local topsoil contribution to airborne particulate matter in the area of Rome (Italy). Source profiles, Atmos. Environ., 69, (2013) 1-14, 2013.

Potts, P. J.: A Handbook of Silicate Rock Analysis, Blackie, U.K., 1987.

R Core Team: R: A language and environment for statistical computing. R Foundation for Statistical Computing, Vienna, Austria, 2013. Available at: http://www.R-project.org/

Rashki, A., Eriksson, P. G., de W. Rautenbach, C. J., Kaskaoutis, D. G., Grote, W., Dykstra J.: Assessment of chemical and mineralogical characteristics of airborne dust in the Sistan region, Iran., Chemosphere, 90, 227ï 236, 2013.

Reid, J. S., Jonsson, H. H., Maring, H. B., Smirnov, A., Savoie, D. L., Cliff, S. S., Reid, E. A., Livingston, J. M., Meier, M. M., Dubovik, O., and Tsay, S. C.: Comparison of size and morphological measurements of coarse mode dust particles from Africa, J. Geophys. Res., 108, D19, 8593-, doi:10.1029/2002JD002485, 2003.

Ritz, C., and Streibig, J. C.: Nonlinear Regression in R, Springer, New York, ISBN: 978-0-387-09615-5, 2008.

Rocha-Lima, A., Martins, J. V., Remer, L. A., Krotkov, N. A., Tabacniks, M. H., Ben-Ami, Y., and Artaxo, P.: Optical, microphysical and compositional properties of the Eyjafjallajökull volcanic ash, Atmos. Chem. Phys., 14, 10649ï 10661, doi:10.5194/acp-14-10649-2014, 2014.

Rudnick, R. L. and Gao, S.: Composition of the Continental Crust, in: Treatise on Geochemistry: Holland, H. D. and Turekian, K. K. Editors, Elsevier, Amsterdam, vol. 3, 1ï 64, ISBN: 978-0-08-043751-4, 2003.

Sarbas, B. and Nohl, U.: The GEOROC database as part of a growing geoinformatics network, in: Geoinformatics 2008ð Data to Knowledge, Proceedings, U.S. Geological Survey Scientific Investigations Report 2008-5172: Brady, S. R., Sinha, A. K., and Gundersen, L. C. Editors, 42-43, 2008. Available at: http://georoc.mpch-mainz.gwdg.de/georoc/Start.asp

Scheuvens, D., Schütz, L., Kandler, K., Ebert, M., Weinbruch, S.: Bulk composition of northern African dust and its source sediments - A compilation, Earth-Sci. Rev., 116, 170ï 194, 2013.

Scheuvens, D. and Kandler, K..: On Composition, Morphology, and Size Distribution of Airborne Mineral Dust, in: Mineral Dust. A Key Player in the Earth System, chapter 2, Pages 15-49. Knippertz, P. and Stuut, K. J.-B. W. Editors, Springer, U.S., ISBN: 978-94-017-8978-3, 2014.

~~Simon, H., Beck, L., Bhave, P. V., Divita, F., Hsu, Y., Luecken, D., Mobley, J. D., Pouliot, G. A., Reff, A., Sarwar, G., and Strum, M.: The development and uses of EPAôs SPECIATE database, Atmos. Pollut. Res., 1, 196ï 206, 2010.~~

Smith, A. J. A. and Grainger, R.G.: Does variation in mineral composition alter the short-wave light scattering properties of desert dust aerosol?, J. Quant. Spectrosc. Radiat. Transfer, 133, 235ï 243, 2014.

Sokolik, I. N. and Toon, O. B.: Incorporation of mineralogical composition into models of the radiative properties of mineral aerosol from UV to IR wavelengths, J. Geophys. Res., 104, D8, 9423-9444, 1999.

Sokolik, I. N., Winker, D. M., Bergametti, G., Gillette, A., Carmichael, G., Kaufman, Y. J., Gomes, L., Schuetz, L., Penner, J. E.: Introduction to special Sect.: Outstanding problems in quantifying the radiative impacts of mineral dust, J. Geophys. Res., 107, D15, 18,015-18,027, 2001.

Stuut, J.- B., Smalley, I., OôHara-Dhand, K.: Aeolian dust in Europe: African sources and European deposits, Quatern. Int., 198, 234ï 245, 2009.

Van Dyck, P., Storms, H., Van Grieken, R.: Automated quantitative electron microprobe analysis of particulate material, Journal de Physique, C2, suppl. au n.2, 45, 781-784, doi: 10.1051/jphyscol:19842179, 1984.

Vermote, E. F., Tanrè, D., Deuzè, Herman, M., Morcrette, J. J., and Kotchenova, S. Y.: Second simulation of a satellite signal in the solar spectrum - vector (6SV), 6S User Guide Version 3, 2006. Available at: http://6s.ltdri.org

Vermote, E. F., Tanrè, D., Deuzè, J. L., Herman, M., and Morcrette, J. J.: Second simulation of the satellite signal in the solar spectrum, 6S: An overview, IEEE T. Geosci. Remote, 35, 675ï 686, doi:10.1109/36.581987, 1997.

Viana, M., Pey, J., Querol, X., Alastuey, A., de Leeuw, F., Lükewille, A.: Natural sources of atmospheric aerosols influencing air quality across Europe, Sci. Total. Environ., 472, 825ï 833, 2014.

Wagner, R., Ajtai, T., Kandler, K., Lieke, K., Linke, C., Müller, T., Schnaiter, M., and Vragel M.: Complex refractive indices of Saharan dust samples at visible and near UV wavelengths: a laboratory study, Atmos. Chem. Phys., 12, 2491ï 2512, 2012.

WCP-112: A Preliminary Cloudless Standard Atmosphere for Radiation Computation. Geneva, World Meteorological Organization, 1986.

White, A. F. and Buss, H. L.: Natural weathering rates of silicate minerals, in: Treatise on Geochemistry, 2nd Ed., Vol 7, Pages 115-155. Holland, H. D. and Turekian, K. K. Editors, Elsevier, Amsterdam, vol. 7, 115-155, ISBN: 978-0-08-043751-4, 2014.

Wilks, D. S.: Statistical methods in the atmospheric sciences, 2nd Ed., Elsevier, Amsterdam, chapter 5, ISBN: 13:978-0-12-751966-1, 2006.

Willis, R. D., Blanchard, F. T. and Conner, T. L.: Guidelines for the Application of SEM/EDX Analytical Techniques to Particulate Matter Samples, US EPA Report n. 600/R-02/070, 2002.

1 Ziebold, T. O.: Precision and sensitivity in electron microprobe analysis, Anal. Chem., 39, 8,
2 858ï 861, 1967.

Table 1. Quality assessment of SEM XEDS microanalysis. ~~% æ are reported as absolute values.~~

	Dust	Mineral particle	K	Na	Ca	Mg	Fe	Mn	Al	Si	Ti
Repeatability (% rsd[a])	Volcanics		10	28	14	19	12	39	6	6	29
	Road dust		35	43	33	23	33	34	36	31	54
	Siliciclastics		15	24	10	13	17	31	11	8	56
	Travertine		17	25	2	25	21	31	14	6	54
Consistency with XRF (% æ[a,b] ± prop. error)	Volcanics		2.4 ± 0.1	55.4 ± 0.1	22.7 ± 0.3	-	32.2 ± 0.1	500 ± 10	15.8 ± 0.2	10.8 ± 0.1	41.4 ± 0.5
	Road dust		37.5 ± 0.3	> 100	28.2 ± 0.1	> 100	37.7 ± 0.7	> 100	22.3 ± 0.2	37.4 ± 0.2	87.6 ± 1.4
	Siliciclastics		22.2 ± 0.1	78.7 ± 2.1	39.2 ± 0.7	52.4 ± 0.3	10.8 ± 0.2	470 ± 10	2.8 ± 0.1	50.7 ± 0.2	7.8 ± 0.5
Accuracy ($g\ cm^{-3}$)		Quartz	-	-	-	-	-	-	-	3.4 ± 0.02	-
		Kaersutite	0.07 ± 0.02	0.04 ± 0.03	0.24 ± 0.02	0.23 ± 0.03	0.67 ± 0.01	0.02 ± 0.01	0.49 ± 0.02	1.12 ± 0.02	0.11 ± 0.02

		Calcite	-	-	4.1 ± 0.02	-	-	-	-	-	-
	Accuracy (% æ[b,c] ± prop. error)	Quartz	-	-	-	-	-	-	-	28 ± 0.4	-
		Kaersutite	37.3 ± 0.6	94.1 ± 18.3	47.4 ± 1.5	38.6 ± 0.3	28.6 ± 0.2	61.5 ± 1.8	28 ± 0.3	6.4 ± 0.3	40 ± 2
		Calcite	-	-	52 ± 1	-	-	-	-	-	-

a. % relative standard deviation

~~a~~b. % æ : absolute percent difference between elemental composition determined by SEM XEDS and ~~Reference term of %æ: bulk~~ elemental composition of same local dust determined by ED-XRF (Pietrodangelo et al., 2013). Prop. err.: propagated error.

~~b~~c. % æ : absolute percent difference between the element %wt in the mineral particle and the element %wt in the bulk ~~Reference term of %æ: bulk elemental composition of~~ standard mineral (EDAX Inc.).). Prop. err.: propagated error.

1

2

Table 2. Average mineral composition (% wt) of dust samples by XRD analysis.

	Volcanic rocks	Siliciclastic rocks	Marlstones	Road dust (Volcanics)	Road dust (Travertine)	Travertine*
Phyllosilicates	57	52	26	7	-	-
Tectosilicates	18	6	0.7	8.7	6	-
Inosilicates	26	-	1.5	22.7	10.2	-
Quartz	4	11	4	1.3	3	-
Calcite	-	31	68	60.3	81	> 90

* After Pentecost (2005)

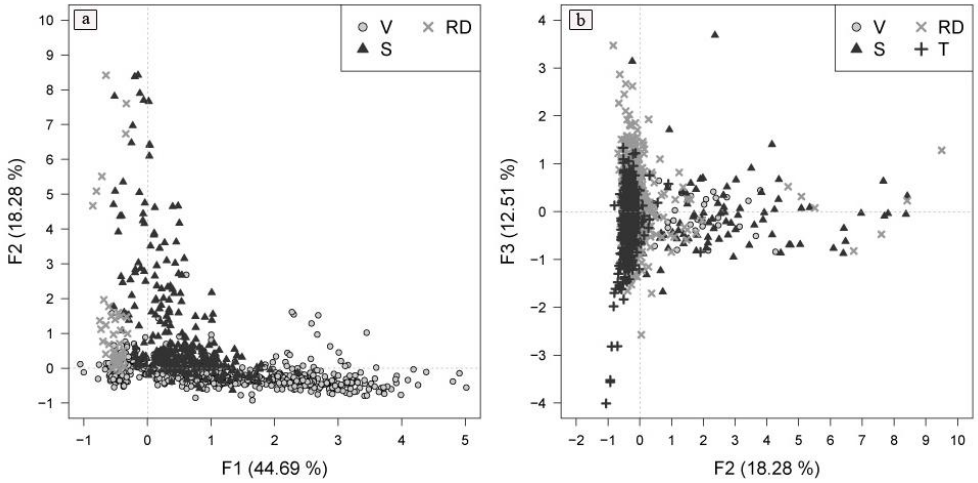

Figure 1. PCA of elemental ratios calculated on individual dust particles composition: score plots of factors (F1, F2, F3) with eigenvalue higher than unity. V: volcanics; S: siliciclastics; RD: road dust; T: travertine.

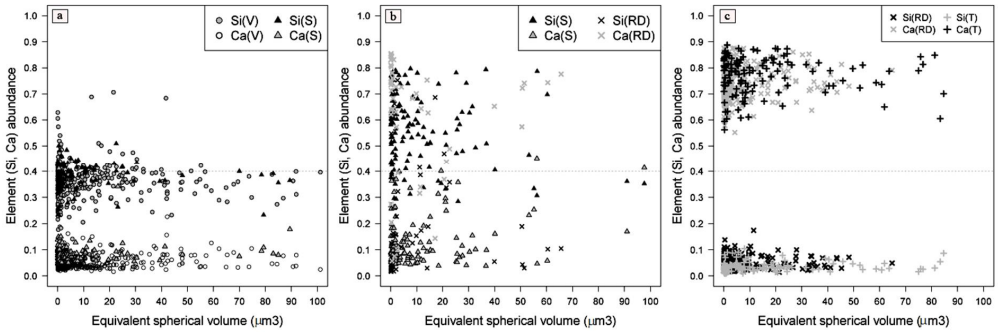

Figure 2. Ca and Si abundances of particles with highest PCA score in F1 (a), F2 (b), or F3 (c), plotted versus the particle equivalent spherical volume.

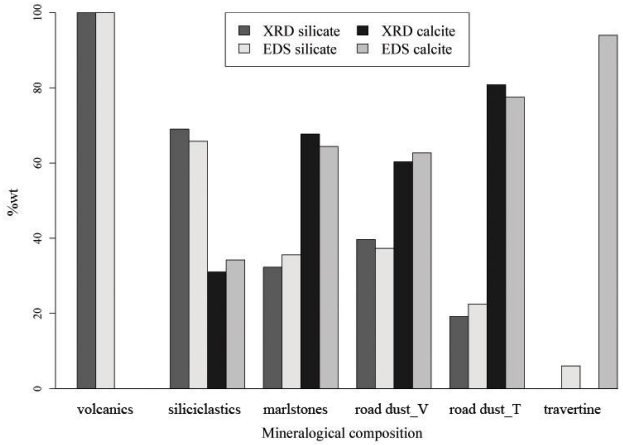

Figure 3. Total silicate (including quartz) and calcite amounts (%wt) of dust samples, obtained by X-ray diffraction bulk analysis and SEM XEDS particle microanalysis.

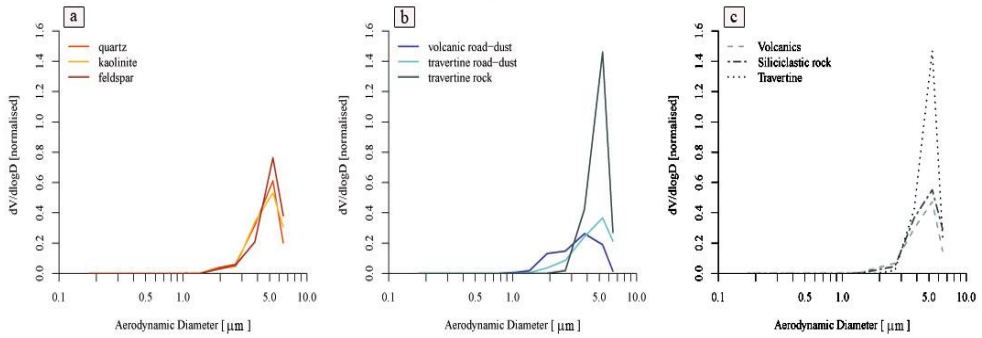

Figure 4. Normalised volume size distributions of most abundant silicates (a), calcite (b), and local dust types (c) in the PM_{10} fraction. Calcite is differentiated by natural (travertine) or anthropic (road dust) origin.

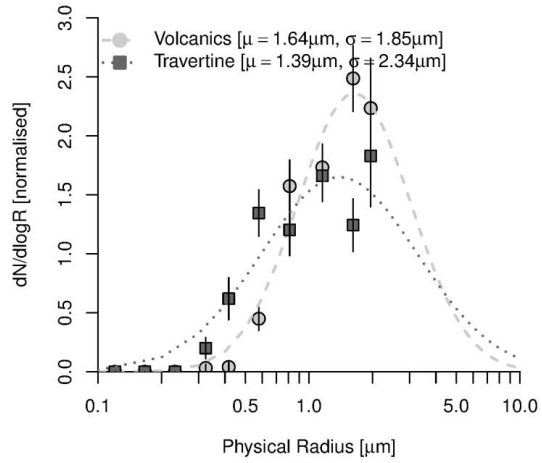

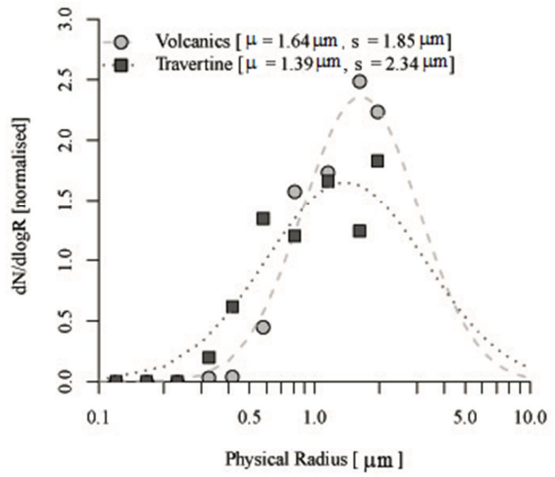

Figure 5. Probability density function fitted to log-normal distribution of the volcanics and travertine PM_{10} dust. Error bars represent uncertainties of bin weight.

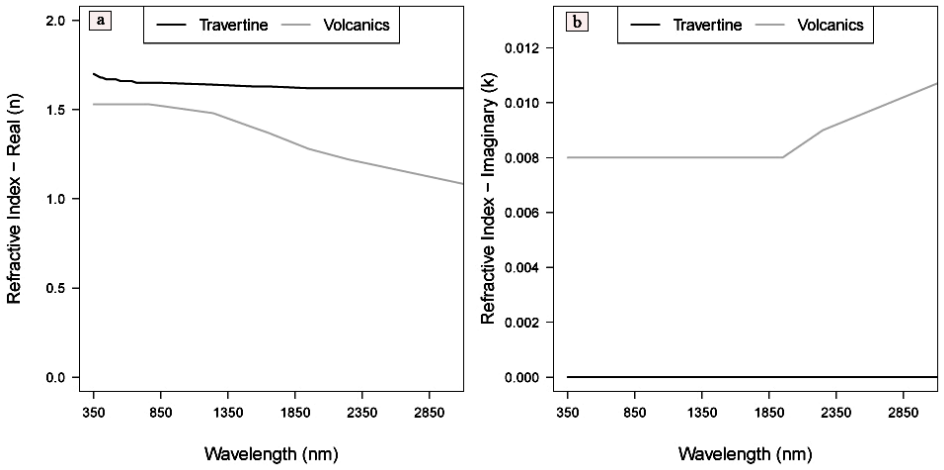

Figure 6. Real (a) and imaginary (b) part of refractive index of the volcanics and travertine PM_{10} dust.

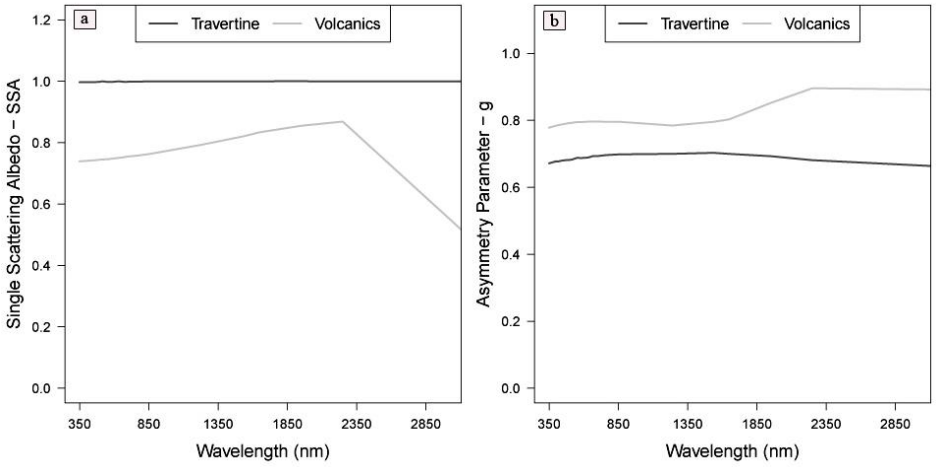

Figure 7. Single scattering albedo (a) and asymmetry parameter (b) of the volcanics and travertine PM_{10} dust.

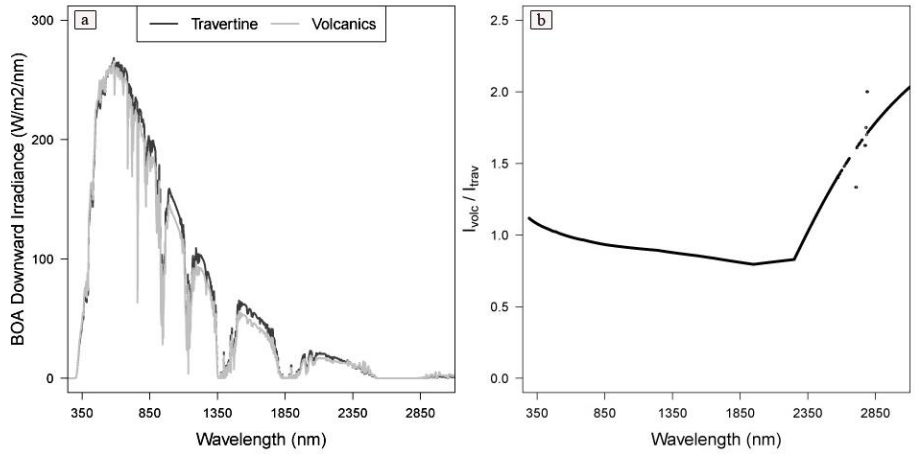

Figure 8. BOA downward solar irradiance (a) of an atmosphere composed by only volcanics, or travertine, PM_{10} dust, and volcanics to travertine irradiance ratio (b).

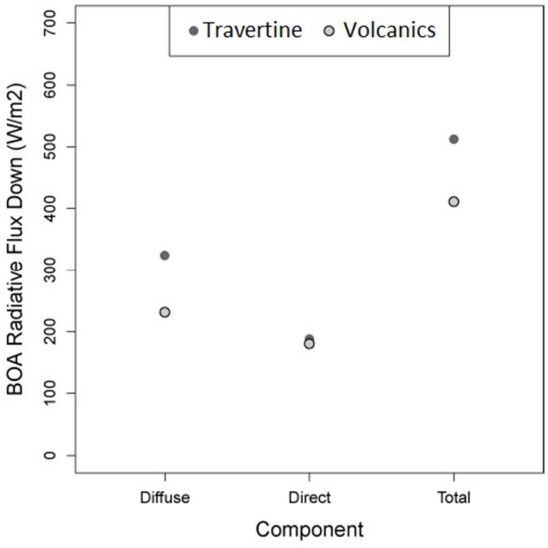

Figure 9. Diffuse, direct and total BOA downward radiative flux (W m^{-2}) over the 250 ï 4000 nm spectral domain, simulated by the 6SV code.

Supplementary materials

Appendix I

Internal standard approach to quantification of particle elemental composition from SEM XEDS microanalysis

First, high-counts spectra of particles analyzed manually in the dust sample matrix (as described in Sect. 2.2) were quantified by the standard-based routine available from EDAX control v. 3.3 package (Newbury and Ritchie, 2013); to this aim, the pure minerals available from EDAX Library have been used as standards. Long acquisition time and high counts of these spectra are expected to minimize the statistical error of quantification (Goldstein et al., 1986). From the EDAX quantification routine, the element Z (atomic number), A (absorption) and F (fluorescence) correction factors, related to the influence of the particulate matrix on X-ray losses of individual particles, are obtained for each analyzed particle of a sample.

Element ZAF mean values, differentiated by dust sample, were then obtained by averaging, within each sample, ZAF values of all analyzed particles. Finally, the sample-specific mean ZAF values were used in the quantification of particle spectra obtained by automated microanalysis. The conventional standard-based ZAF-corrected Castaingôs method was used also in this case; however, the standard element concentration and ZAF were those of the manually-analyzed particles. By this procedure, indeed, manually analyzed particles could be assumed as internal particle standard, on a sample-specific base. The reliability of quantification of manually analyzed particles, by Castaingôs first approximation approach, was evaluated in terms of accuracy with respect to mineral standards available from the EDAX Library. Details and results are discussed in Sect. 3.1.1.

Particles showing total ~~sum of element percent weight (%wt~~percent weight (%wt) of the particle that could be identified~~)~~ below 50 (including oxygen estimated by element oxides) were not further considered in the rest of the study.

Reference XEDS spectra and elemental composition of pure minerals, to be used for particle allocation, were obtained either from the EDAX Library (biotite, clorite, calcite, diopside, kaersutite, olivine, plagioclase and quartz) or by the RRUFF project (Downs, 2006) and GEOROC (Sarbas and Nohl, 2008) open-source databases, available on the web. Minerals collected from Central Italy were preferred where possible.

Spectral matching was performed by the chi-square test for spectral goodness of fit included in the Library matching v.3.3 application (EDAX Inc., 2000). In cases where spectral matching couldnôt be performed, allocation of particles to mineral species was obtained on the basis of the best fit of the dust particle %wt element composition versus the composition of pure minerals, by single linear regression analysis (SLR). The reliability of the internal standard approach has been evaluated by assessing the consistency of the allocation to mineral species (which directly depends on results of quantification by internal standard approach) with XRD analysis.

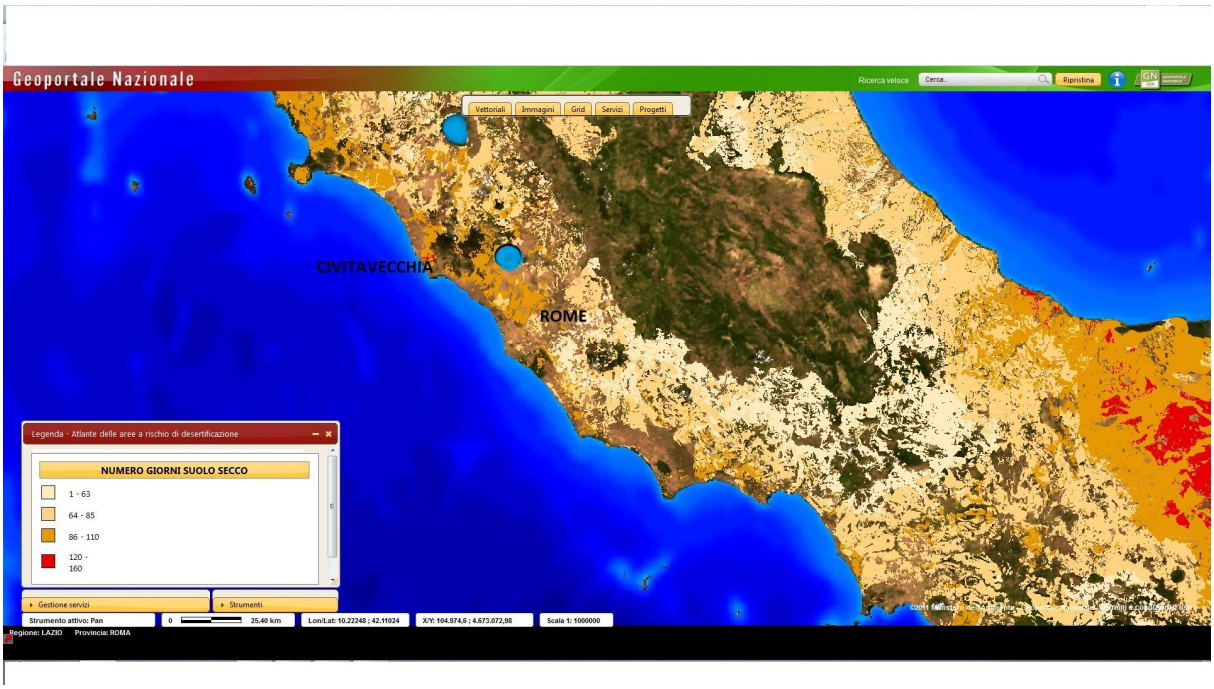

Figure 1S. Map of the annual average number of dry soil days in the area of study of this work (Geoportale Nazionale MATTM, 2011). Highest number of dry soil days (86 ÷ 110) is observed in the northern zone of the study area of this work.

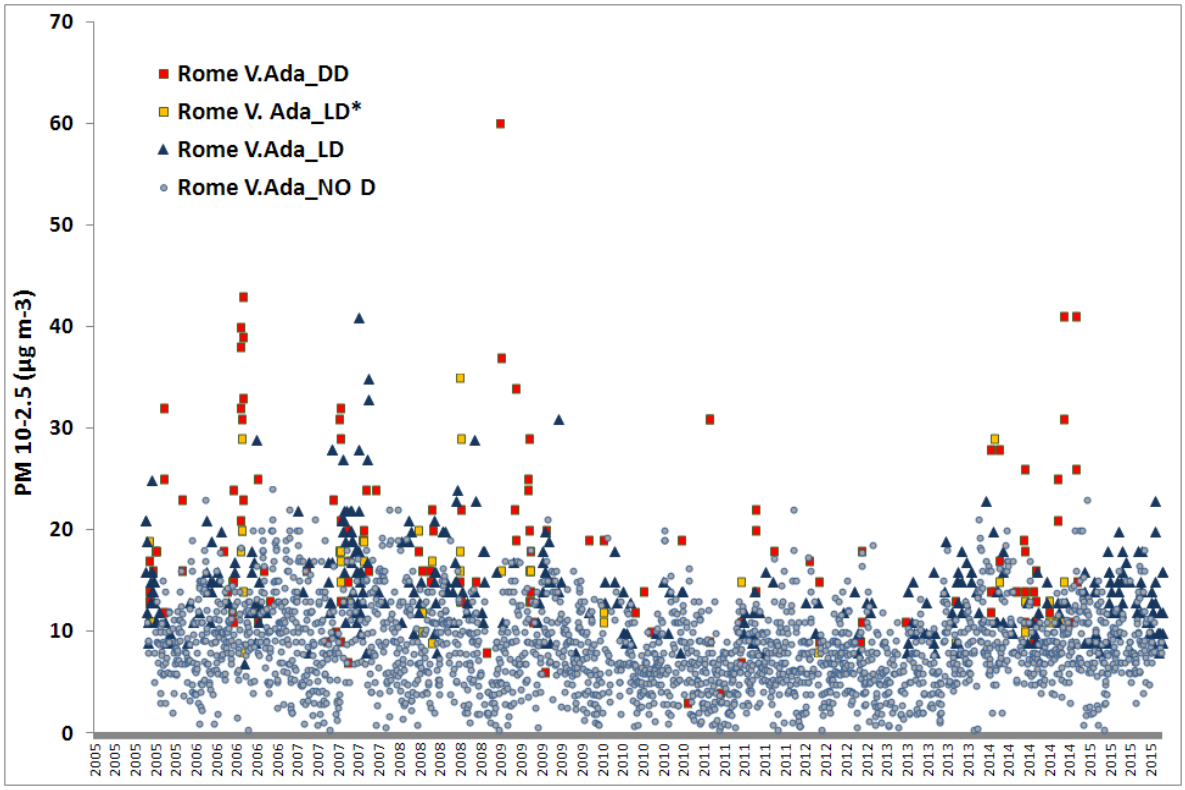

Figure 2S. Daily coarse PM at Villa Ada site (urban background) in Rome, along the 2005 ï 2015 period. Data in the plot refer to days of: desert dust intrusion at-ground (DD), local crustal contribution occurring next a DD intrusion event (LD*), local crustal contribution distant from DD events (LD) and low crustal contribution (NO D).

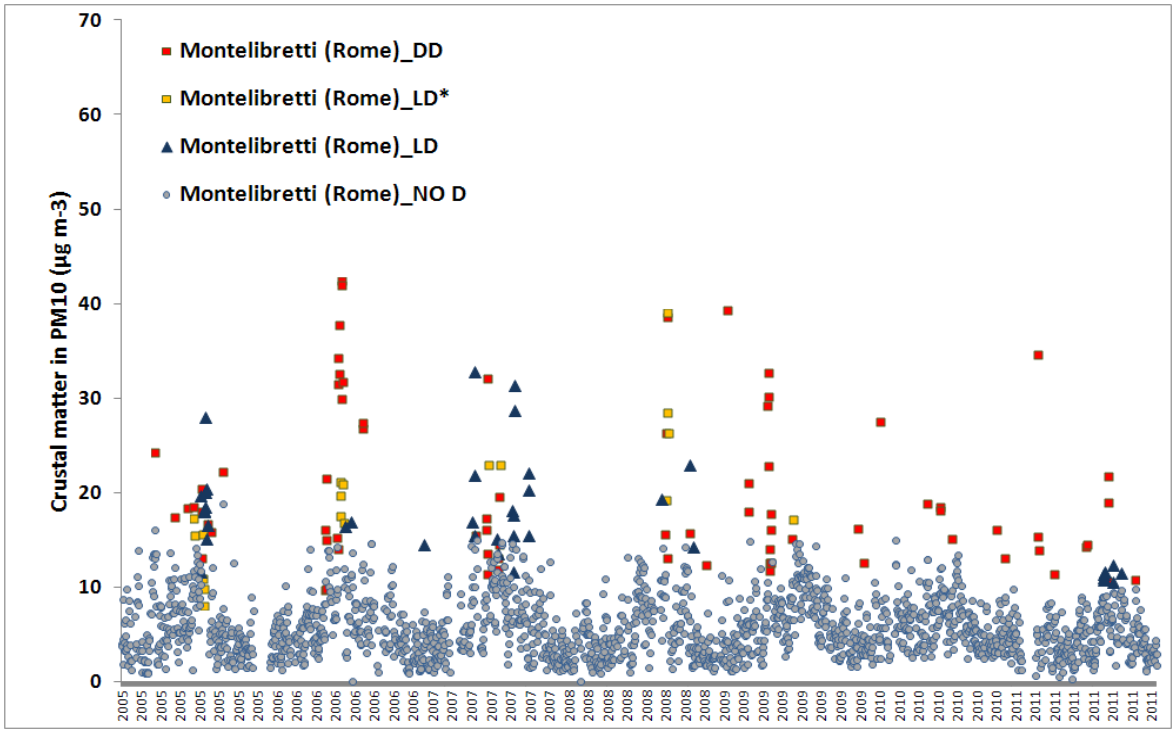

Figure 3S. Daily crustal matter in the PM10 at Montelibretti (EMEP site), in Rome skirts, along the 2005 ï 2011 period. Data in the plot refer to days of: desert dust intrusion at-ground (DD), local crustal contribution occurring next a DD intrusion event (LD*), local crustal contribution distant from DD events (LD) and low crustal contribution (NO D).

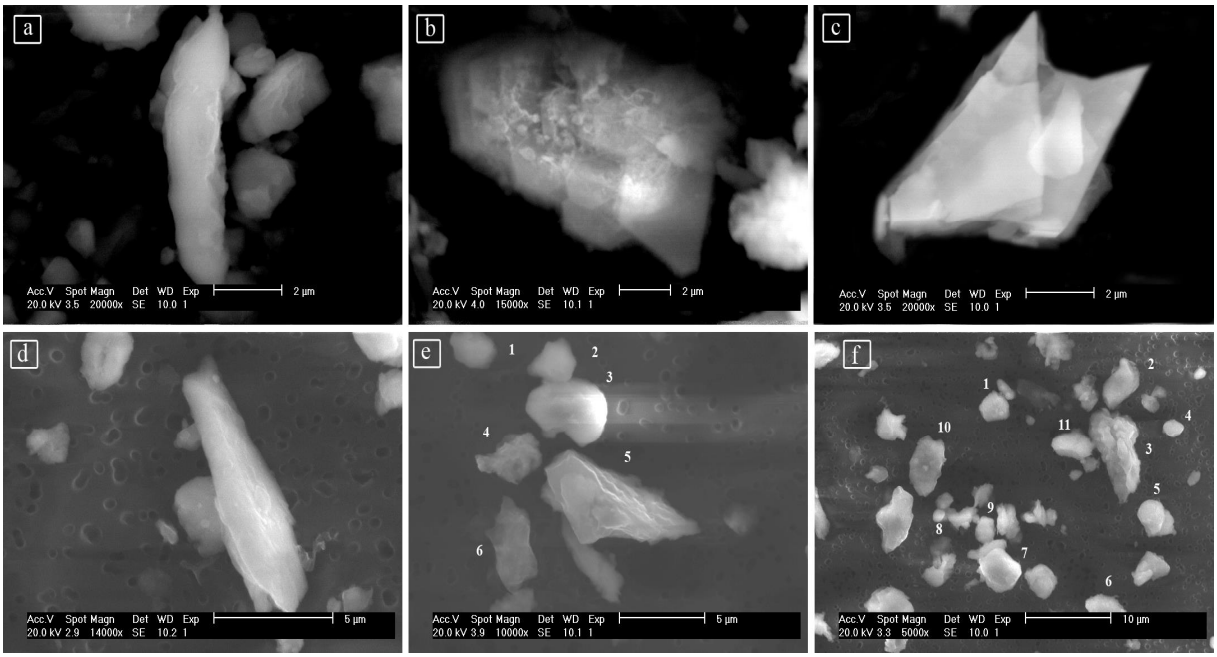

Figure ~~2S~~3S. SEM micrographs of mineral particles identified in the study area.

Instrumental conditions are reported on each micrograph. a: Diopside; b: Mica; c: Montmorillonite; d: Muscovite; e: Calcite (particle #: 1, 2, 3), Talc, K-feldspar and Quartz (respectively, particle #: 4, 5, 6); f: Calcite (particle #: 1, 6, 7, 9), Quartz (particle #: 3, 5, 8, 10), Chabazite (particle #: 4, 11), Muscovite (particle # 2).

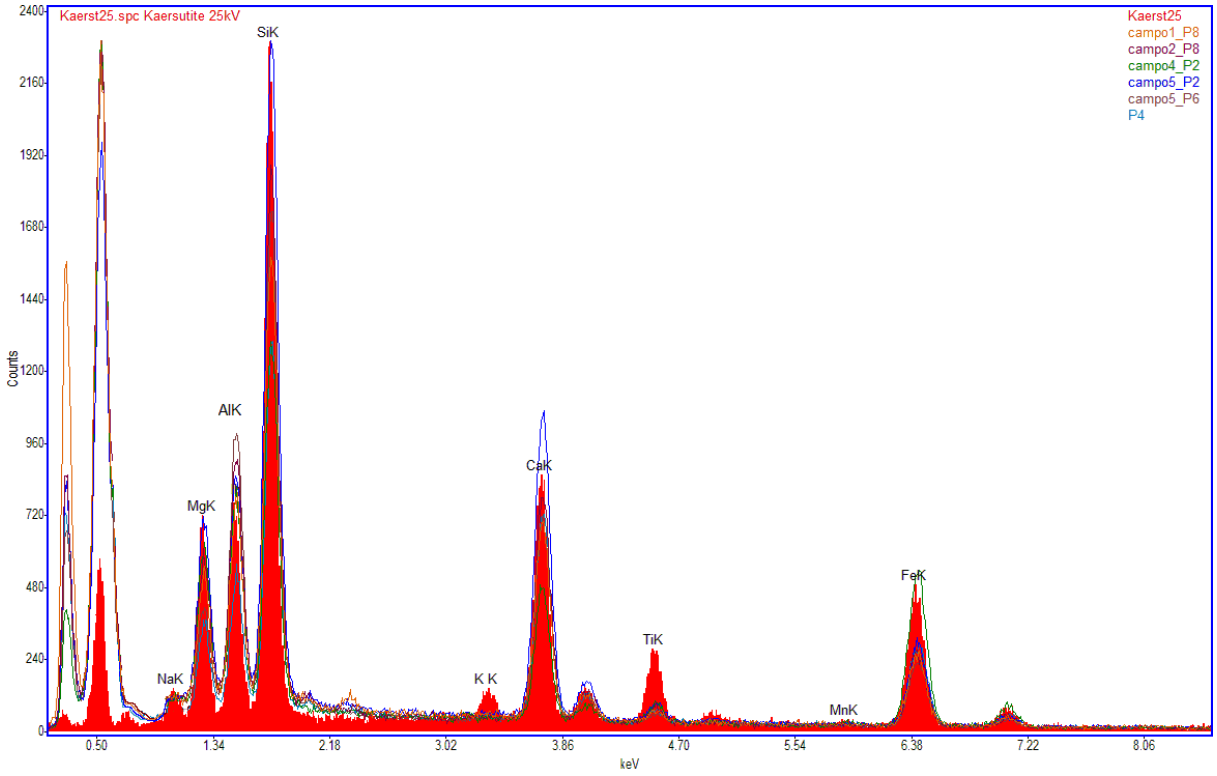

Figure ~~3S~~4S. Overlap of high-counts XEDS spectra of particles classified as Kaersutite, with respect to the EDAX spectrum of the bulk mineral standard.

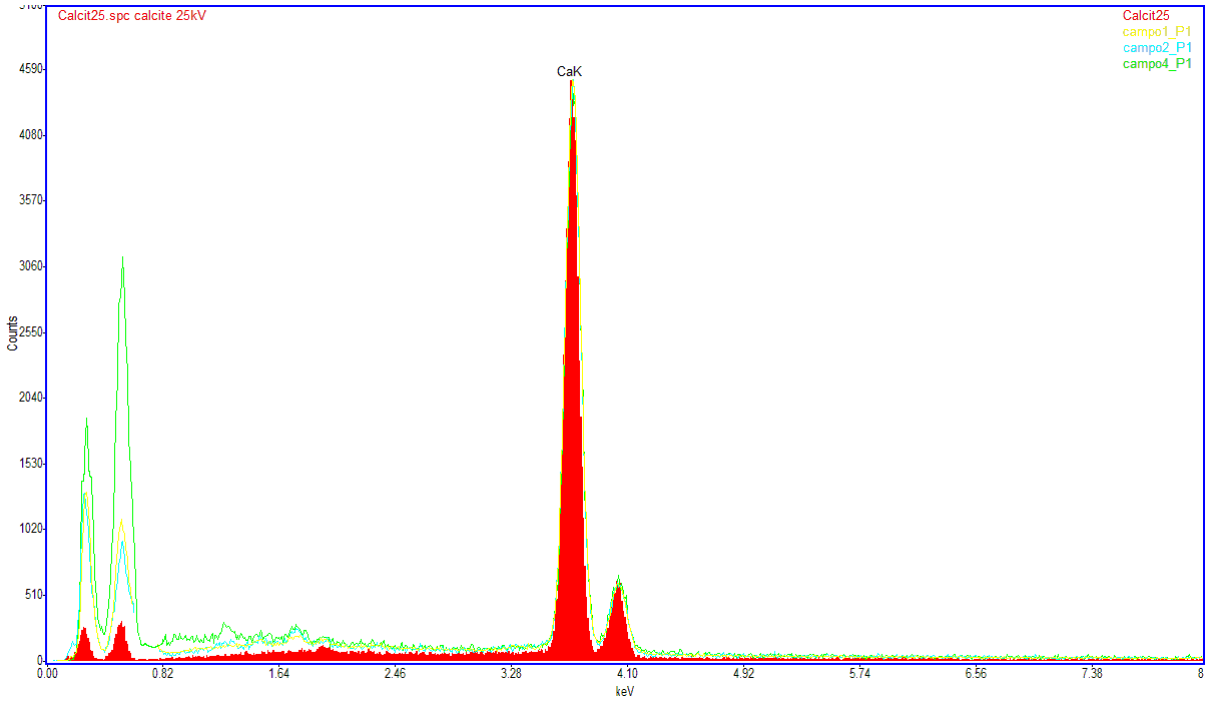

Figure ~~4S~~5S. Overlap of high-counts XEDS spectra of particles classified as Calcite, with respect to the EDAX spectrum of the bulk mineral standard.

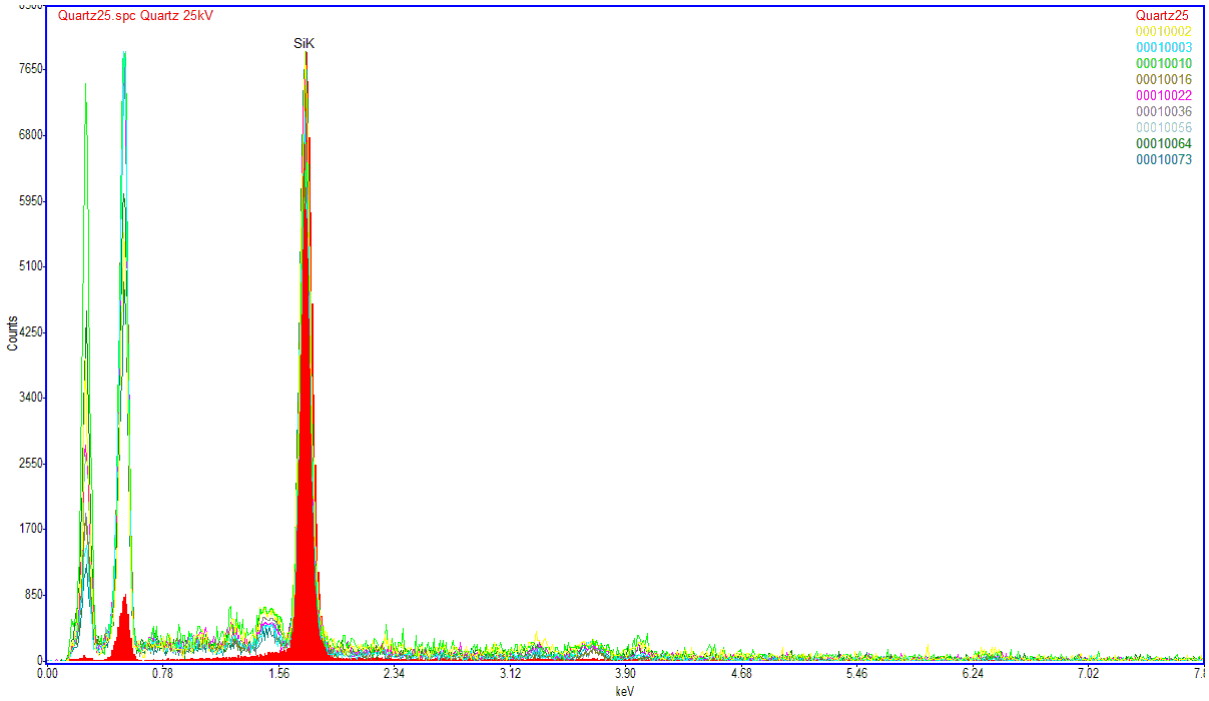

Figure ~~5S~~6S. Overlap of high-counts XEDS spectra of particles classified as Quartz, with respect to the EDAX spectrum of the bulk mineral standard.